10. EARTH OBSERVATIONS AND PHOTOGRAPHY

EXPERIMENT MA-136

Farouk El-Baz[a†] and D. A. Mitchell[a]

ABSTRACT

The Gemini, Apollo, and Skylab missions showed that orbiting astronauts can provide valuable data composed of visual observations and photographs. For this reason, the primary objectives of the Earth Observations and Photography Experiment of the Apollo-Soyuz Test Project were to photograph various terrestrial structures and to use the capabilities of man as a trained observer in visually studying Earth features and phenomena. Man's special capabilities include the sensitivity of the eye to subtle color variations and the speed with which the eye-brain system can interpret what is seen and select targets for photography.

Real-time astronaut observations constitute a useful complement to orbital photographs and greatly aid in their interpretation. Targets for mapping and hand-held photography were selected on the basis of their value to specialists in the Earth sciences including geology, oceanography, desert study, hydrology, meteorology, and environmental science.

INTRODUCTION

Background

The experiences of the Gemini, Apollo, and Skylab Programs proved that scientifically interesting features can be selected and photographed by observers in space. Photographic records of these programs include a plethora of valuable scenes taken from orbital altitudes, both from Earth orbit (e.g., refs. 10-1 to 10-4) and from lunar orbit (e.g., refs. 10-5 to 10-7).

During the Apollo Program, it became apparent that the orbiting astronauts could see more than what was recorded on film. To test this capability, plans were made, beginning with the Apollo 13 crew, to train Moon-bound astronauts to make visual observations. However, because the Apollo 13 mission was aborted, the first attempt at making visual observations from lunar orbit was made on Apollo 14. The results were encouraging (ref. 10-8), and a program was developed for the systematic acquisition of scientifically relevant data on Apollo 15 (refs. 10-9 and 10-10), Apollo 16 (refs. 10-11 and 10-12), and Apollo 17 (refs. 10-13 and

---

[a]National Air and Space Museum, Smithsonian Institution.

[†]Principal Investigator.

10-14). Emphasis was placed on the command module pilot (CMP) of each Apollo mission because he spent more time in lunar orbit than did his crewmates. Also, premission training and data acquisition were limited to the field of lunar geology during the Apollo missions.

The Skylab Program provided the first opportunity to pursue a systematic visual study of the Earth. However, this study was done only on the last of three missions, Skylab 4. Because of the nature of the Earth, the Skylab visual observations program included geology, oceanography, hydrology, meteorology, etc. (ref. 10-15). The long duration of the mission (84 days) allowed repeated observations of the same area and during different seasons. Observations on Skylab 4 and their documentation with photographs proved to be a very worthwhile effort and resulted in significant findings (ref. 10-15). During the Apollo-Soyuz Test Project (ASTP), selected features of interest from the Skylab Earth observations program were reexamined and viewed from a different altitude, 2 years later in time.

Visual Observation Team

To assist in the planning and implementation of the ASTP Earth Observations and Photography Experiment, a team of experts in the fields of geology, oceanography, desert study, hydrology, meteorology, and environmental science was assembled. The Earth observations team (table 10-I) was composed of 42 individuals, including the Principal Investigator (PI) and 12 Co-Investigators (Co-I). The responsibilities of this team of experts and support personnel were as follows.

1. To collect and compile problems to be solved in support of ongoing research in the Earth sciences.

2. To evaluate and select achievable goals based on experience and level of crew training.

3. To recommend and pursue a training program of mutually acceptable procedures and sites.

4. To identify Flight Plan requirements and tools necessary to achieve the objectives.

5. To support the mission operations for nominal and contingency flight plans.

6. To report the results and the possible applications to future space flight.

Earth Observation Sites

The primary objective of the ASTP Earth Observations and Photography Experiment was to use the Apollo and Skylab experiences in acquiring photographs of specific Earth features, processes, and phenomena and in making visual observations from orbit to complement photographic data. Visual sightings are needed because the extensive dynamic range and color sensitivities of the eye cannot be matched by any one film type and also because, in special cases, on-the-scene interpretations of obscured features and phenomena are necessary.

To achieve the primary objective, both photographic mapping and visual observation sites were included in the Flight Plan. A total of 11 mapping sites (table 10-II) and 12 visual observation sites (fig. 10-1) were selected. The 12 visual observation sites were chosen according to geographic localities and included 60 specific targets of prime scientific interest (table 10-III). This method of target identification made it possible for both planners and astronauts to easily discuss and locate targets selected for scientific investigations.

Crew Training

One of the main objectives of the Earth Observations and Photography Experiment was to utilize the capabilities of man as a trained observer in orbit. In accordance with this goal, an extensive training program consisting of classroom sessions and flyover exercises was initiated 1 year before the mission.

Classroom training was conducted by Earth scientists from various disciplines. These specialists briefed the astronauts on the types of Earth features they would observe from orbit. The first lectures on geology, hydrology, oceanography, desert studies, and meteorology consisted of background on theory and familiarization with terminology. Subsequent lectures were scheduled on the basis of crew interest. Other sessions, conducted mainly by the Principal Investigator, covered (1) operational procedures and viewing conditions and constraints and (2) groundtrack familiarization and specific photographic and observational requirements. The crew received approximately 60 hours of classroom training during 20 sessions. A schedule of the training sessions is given in table 10-IV.

The flyover exercises were designed to give the astronauts practical experience in target acquisition and site selection and to familiarize them with the types of features they would observe from Earth orbit. The astronauts were also able to practice verbalizing about and handling onboard equipment, including cameras, lenses, the color wheel, and the tape recorder. Each flyover exercise consisted of a predetermined flight route with a visual observations book designed for that particular flight and similar to the one to be used during the actual mission. Seven high-altitude flyover exercises (table 10-V) were planned over areas of the United States. The California flyover was repeated twice and the Florida flyover once for a total of 10 flyover exercises. During these flights, the astronauts observed both sites scheduled for observation during ASTP and examples of the various types of ocean features and landforms they would view from Earth orbit.

These flyovers were valuable in showing the astronauts how to select the optimum conditions for observations and photography. For example, they found that sunglint was especially important in observing ocean features such as currents, eddies, and internal waves. On land, high Sun angles were best for observing color variations, whereas a low Sun angle enhanced relief and facilitated observations of faults and sand dunes. The flyover exercises gave the crew valuable practice in making visual observations and acquiring photographs.

METHODS AND TECHNIQUES

Photographic Systems

Three types of imaging systems (video, cameras, and scanners) have been successfully used in Earth-orbital surveys. The ASTP photographs of observation and mapping sites were made with a video tape recorder (VTR), a 70-millimeter Hasselblad reflex camera (HRC), a 70-millimeter Hasselblad data camera (HDC), a 35-millimeter Nikon camera (with exposure control), and a 16-millimeter data acquisition camera (DAC).

The 70-millimeter HDC was usually bracket mounted and could accept both 60-millimeter and 100-millimeter lenses. An intervalometer was used, and the frequency of frame usage was calculated to provide stereoscopic coverage with a 60-percent overlap. The HDC was equipped with a reseau plate to improve geometric accuracy and to allow the construction of controlled photomosaics. In general, the photographs obtained with the HDC are excellent, with the exceptions of a few short segments of unplanned photography that were out of focus and one mapping pass over the northeastern United States in which the wrong lens was used.

In addition to mapping strips, photographs of approximately 60 observation sites were made using either the hand-held HRC with the 50- or 250-millimeter lens or the HDC. However, most of the visual observation targets were photographed with the HRC. The HRC has a single lens reflex mechanism that allows the astronaut to see what he is photographing. The crew reported that light loss through the 250-millimeter lens made it difficult to locate the target and to center it within a frame. However, all photographs taken with this lens are excellent. The 16-millimeter DAC was used to acquire photographic data over the western Sahara and to provide a sequential film of color zone transitions in the largest sand sea in the world.

Real-time television transmissions were also scheduled, and images of the daylight portion of revolution 124 over the Pacific Ocean were recorded on the VTR. These color television images of the Earth are potentially capable of providing new data in poorly studied areas and in areas such as the Pacific Ocean, which is too vast for conventional oceanographic surveys. They can give scientists an astronaut's perspective of target acquisition and tracking and also provide imagery that can possibly be reformatted for stereographic and radiometric analysis.

Thirteen magazines of color film were used for the scheduled mapping sites (type SO-242) and observation targets (type SO-368). The SO-368 film was specially coated with the equivalent of a Wratten 2A filter to improve the color sensitivity of the film by eliminating the effects of short wavelengths. Two magazines of type 2443 color infrared film were also used to facilitate identification of features such as volcanic rocks and red tide blooms.

Visual Observation Aids

The human eye-brain system is similar to a camera in that it has a lens and an iris, it generates images with good resolution and geometric fidelity (the resolving power of the unaided human eye is 0.0003 radian or approximately 0.60° (ref. 10-9)), and it is sensitive to electromagnetic radiation in the visible region. Under laboratory conditions, the eye is estimated to be able to distinguish 1×7.5^6 color surfaces, a precision that is 2 to 3 times better than most photoelectric spectrophotometers (ref. 10-16).

The eye can easily distinguish subtle color variations to a greater extent than any commercially manufactured film, but the brain cannot recall these after a given period of time has elapsed. Real-time calibration of desert and water colors was achieved by the use of a two-sided color wheel composed of carefully selected Munsell colors (fig. 10-2 and table 10-VI). These colors can be compared to the photographs to apprise users of the color sensitivity and fidelity of the film. However, the crew indicated that it was sometimes difficult to make good comparisons because variable lighting conditions inside the spacecraft often resulted in the color wheel being in the shade.

To assist in the acquisition and location of visual observation targets, the use of 20-power binoculars was originally planned. However, after the crew tested the binoculars during flyover exercises, a change was made to use a 16-power monocular. The crew believed the monocular would provide a more convenient means of checking the eye's resolution and of locating targets. During postmission evaluation, the astronauts indicated that the usefulness of the spotting scope was curtailed by the speed with which a target passed outside their field of view.

The principal onboard aid was the "Earth Observations Book." This book was divided into three major sections. The first section contained (1) a time line summarizing the visual observation tasks and mapping camera configurations and (2) a stowage list and a review of operational procedures. Information in the second section pertained to specific visual observation targets and was arranged according to site numbers. For each site, there was a summary page with a map showing revolution groundtracks followed by a page (one for each target) that included specific questions, appropriate diagrams and photographs, and camera settings. The last section was a reference appendix that included maps of the distribution of volcanoes, ocean currents, July cloud cover, etc., and diagrams of various Earth features such as drainage patterns, ocean phenomena, dune types, and faults.

Flight Planning

Earth observations and photography mission tasks required approximately 12 hours of crew time. These tasks were planned during 24 revolutions and assigned to specific crewmembers. The task assignments for the mapping sites and the visual observation targets are listed in table 10-VII.

Planning for the ASTP mission also included simulations of real-time activities. The Earth observations team participated in three mission simulations to practice interaction with other Mission Control Center personnel and with the

crew. These proved to be very useful exercises because the need existed for verbal communications with the astronauts during the mission. The Earth observations team supported the mission and was in contact with ground-truth data collection parties on a 24-hour basis throughout the mission.

RESULTS

Ground-Truth Data

During the real-time operations of the ASTP mission, the largest air, sea, and ground support team of any manned mission collected ground truth to expedite the postmission interpretation of orbital observations and photography (fig. 10-3). This support included the acquisition of metric and multispectral photography by high-altitude aircraft. Aerial photography was acquired simultaneously during several ASTP photographic passes to link ground-based studies with Earth-orbital observations. Ocean research vessels obtained data on sea surface temperatures, salinity, water color, current directions, and cloud types and heights. On land, ground-truth teams collected data to support geological, hydrological, and desert research projects in India, Guatemala, Mexico, the United States, and Egypt. A summary of the reported support operations follows.

ANZUS Eddy (site 11D).- The Australian ship Bombard, stationed in the Tasman Sea, surveyed the warm water ANZUS (Australia-New Zealand-United States) Eddy. Oceanographic data indicated that the nearly circular eddy was 145 to 160 kilometers in diameter with surface temperatures 2° warmer than the surrounding water. Ship personnel also reported a cumulus cloud formation over the center of the eddy and a number of trawlers fishing for tuna within the eddy.

Caribbean (site 7G).- To support crew observations and photography of the extent of organic acid outflow from the Orinoco River, the Bellairs Research Institute of McGill University sponsored three cruises from the island of Barbados on July 21, 22, and 23. Observations and measurements were made of sea state, water color, sea surface temperature, salinity, chlorophyll content, cloud cover, and wind speed and direction.

Egypt (sites 9E and M7).- For the revolution 71 mapping pass over Egypt, geologists from the Ain Shams University in Cairo will provide ground-truth data to be used in support of a photogeological investigation of the Western Desert of Egypt. Field work will be carried out at Abu Râwash, Oweinat Mountain, and the Faiyûm, Baharîya, and Farâfra Oases (fig. 10-4). Ground investigations include detailed mapping, characterization of the structural and topographic setting, and studies of desert erosion patterns and grain transportation. The major objective is to use the geological data in verifying color zonation and other features recorded on the ASTP film.

England (sites 6A and 6B).- The Royal Air Force flew a 3-day sequence over ocean waters off southern Ireland and England. Expendable bathythermographs (XBT's) were dropped from the planes to provide data on water temperature as a function of depth.

Gulf of Mexico (site 5A).- The National Oceanic and Atmospheric Administration (NOAA) research vessel Virginia Key made a transect of the Gulf of Mexico from Miami to the Yucatan peninsula and obtained data on the location of the Gulf Loop Current. Approximately 20 NOAA ships were also stationed around the Mississippi River Delta.

New Zealand (site 1).- The Royal New Zealand Air Force flew P-3 airplanes along the revolution 17 groundtrack starting from East Cape, New Zealand, then north-northeast over the Pacific Ocean to obtain photographic data and to plot cloud types and heights. A New Zealand Navy research vessel made a transit along the same line and acquired oceanographic data, including water temperatures and sound velocity measurements.

Strait of Gibraltar (sites 9K and 9J).- The U.S. Navy research vessel Kane obtained oceanographic data along a line paralleling the revolution 73 groundtrack from the Canary Islands to Spain. These data were obtained to support crew observations of a current boundary extending north and south off the western coast of Portugal. The Navy also flew a P-3 aircraft along this line dropping XBT's. East of the strait in the Mediterranean Sea, the carrier U.S.S. Kennedy obtained oceanographic and meteorological data.

United States (sites 2A, 4A, 4B, 5B, 5E, and 5F).- Several high-altitude flights were flown over the United States with a B-57 aircraft based at the NASA Lyndon B. Johnson Space Center and a U-2 aircraft based at the NASA Ames Research Center. Metric and multispectral photography was obtained with a metric RC-10 camera and a multispectral Vinten System A camera. Sensor data are provided in table 10-VIII. Photographic coverage was acquired over the East Coast (coastal areas of New York, Massachusetts, and Maine), Florida (coastal areas), the northwestern United States (Washington, Idaho, and Oregon), and the southwestern United States (from Kingman, Arizona, to Santa Maria, California).

In addition to the aircraft support, ocean research vessels made measurements in the Gulf Stream and along the New England coast. The U.S.S. Preserver collected data in the Gulf Stream north of Jacksonville, Florida, on the distribution, size, and velocities of eddies. The ship also released four drifting buoys that had transmitters to the Nimbus-F satellite. The buoys were positioned about once a day throughout the mission and provided data on current direction and velocity.

In New England, two Bigelow Laboratory research vessels (the Bigelow and the Challange) made a traverse of the Gulf of Maine from Portland to the Bay of Fundy and also southward to Cape Cod. Data were obtained on the size, shape, and location of red water patches due to toxic phytoplankton and included measurements of sea surface temperature, salinity, chlorophyll content, and water color. In addition to the red tide observations off the coast of Maine, support ships and sampling stations of the Commonwealth of Massachusetts acquired water color, salinity, and biological content data. A high chlorophyll content in the coastal waters off New England was reported and was possibly the result of abnormally heavy rains carrying an increased amount of biota into the sea.

Mission Data

A total of 11 mapping passes and 60 visual observation sites was scheduled. Only one mapping pass was canceled (on revolution 15/16) because of problems in the Flight Plan. Approximately 20 percent of the 100 planned observations of the 60 sites were not performed because of bad weather, making the overall success measure of the experiment approximately 80 percent. The summary results of the photographic mapping sites and the visual observation targets are given in tables 10-IX and 10-X, respectively.

DISCUSSION

The quality of photographic data obtained in previous Earth-orbital surveys has firmly established their value as basic tools in the evaluation of terrestrial features and in the reconnaissance of remote locations. Before the ASTP mission, several types of photographic systems were successfully used in spacecraft. On the Skylab missions, the Earth resources experiment package included a multispectral array of six cameras (with various film/filter combinations in the visible and infrared) as well as a high-resolution Earth terrain camera.

Two of the more obvious advantages of such orbital systems over aerial photography are the large regional coverage and the speed with which data can be obtained. These advantages facilitate the preparation of base maps because mosaics of large areas can be rapidly prepared with orbital photographs. The ASTP planning for visual observations and photography utilized these advantages to their maximum. For example, several mapping passes were scheduled over areas where general land surveys (including a classification of terrain, mineral resources, and land use) are either nonexistent or inadequate. Targets were also selected for photography in oceans and deserts, where size and inaccessibility make conventional surveys impractical.

The large regional coverage of orbital photographs also provides a more efficient method for the observation of large-scale phenomena, such as color transitions within deserts and ocean currents. Orbital photographs have a greater perspective and are useful in the study of broad distributions and regional structure; two examples are major fault zones (such as the San Andreas system and the Levantine Rift) and snow cover and drainage patterns (as in the Cascade Mountains). One other advantage is the stability of spacecraft as a platform for Earth-looking photography. Variations in velocity and attitude are minimal and flightpaths can be determined with great precision. The following is a discussion of some of the ASTP tasks and results in the fields of Earth science selected for emphasis on this mission.

Geology

Geological investigations on the ASTP mission included observations of major active fault zones, river deltas, volcanoes, and astroblemes (ancient impact scars). Studies of global tectonic patterns were made by observation and photography of some major areas of continental crustal fracturing. One of these areas

was the Levantine Rift, a fault complex formed as a result of the motion of the Arabian subplate. The crew was asked to observe the northern extensions of this rift and to obtain photographs necessary to an understanding of the locations and mechanisms of displacement. Excellent photographs were obtained of the entire area (e.g., fig. 10-5). The photographs support the theory that motion of the Arabian subplate is counterclockwise drift rather than eastward rotation. Astronaut observations of the area provided additional data:

> The one thing I noticed was that if you look at the 9G map [fig. 10-6], the dotted line on the left up near the end of it, makes a bend to the left and follows a new tectonic line or fault which goes along parallel to the Turkish coast. In other words, the one on the left, number 1, goes up . . . and then makes a left turn and parallels the Turkish coast. Two seems to be obscured and it just ends in a lot of jumbled country up somewhere slightly beyond where the number 2 is, and it seems to end right in this jumbled area. Three, I could trace clear up to a river which - I'll have to see a map later. But I could trace the faults out, going rather eastward. You could see them through the valley silt, clear up to a river which must be inland in either Syria or Turkey. So the overall pattern of these is a fan; three going almost eastward, and one bending finally to the north, and two going to the northeast. (CMP)

Photographs of river deltas were also acquired. In the geologic record, deltaic sediments are often a source of natural gas and oil accumulation; an understanding of the growth of deltas might have applications in the future development of these resources. Several major river deltas were photographed, including the Orinoco (fig. 10-7), Rhone, Nile (fig. 10-8), Fraser, Danube, and Yellow Rivers. These photographs will be compared with previous orbital photographs in an effort to document the rate and direction of growth of modern deltas.

A study was also made of astroblemes, or ancient impact scars, to increase knowledge of the interaction of the Earth and meteoritic bodies and to locate new areas for possible economic exploitation. Photography of this type of feature was obtained in Libya near the Kufra Oasis (fig. 10-9). Resolution was excellent. The central dome and ghost ring of one known feature, the BP structure, were easily recognized. Another circular feature, possibly a twin site, was also identified.

Oceanography

In the field of oceanography, a study was made of major ocean features such as eddies, currents, and internal waves. Because large areas can be rapidly surveyed, the global view of oceans from space is especially useful. As previously stated, extensive ground-truth data collection (fig. 10-3) was coordinated with

photographic passes to aid in postmission data interpretation. Areas of prime scientific interest include the following.

Area	Interest
Coral Sea	Interaction of currents with the Great Barrier Reef Eddies in the Coral Sea
ANZUS Eddy	Support of an Australian-New Zealand-United States oceanographic study of a 200-kilometer-wide eddy east of Sydney, Australia
Caribbean Sea	Ocean currents and their relation to fisheries Eddies and their relation to the Gulf Stream
Gulf of Mexico	Development of the Gulf Loop Current Eddies and currents in the Yucatan Channel
Mediterranean Sea	Observation and photography to support oceanographic study by U.S. Sixth Fleet research team Effects of reduction of freshwater from the Nile River

Investigations of these features will provide a better understanding of dynamic ocean phenomena and will have potential applications to trade, shipping, and the identification of environmental parameters affecting fisheries.

The crewmen remarked that the ease with which oceanographic targets were discerned was a function of several factors; Sun glitter was identified as the most influential parameter. For example, the following remarks concerned the visual identification of internal waves west of the Strait of Gibraltar (fig. 10-10):

> I was looking for all these things and suddenly they popped out within a second right there. Just suddenly when the Sun angle changed, everything was there, the waves and the boundary were all there and we just snapped a series on them. But before that, there was nothing but just solid blue water and then they just suddenly popped . . . You have to be ready and the Sun angle has to be just right. And it's there for just a short period of time and then it's gone. (ACDR)

A study was also made of red tide occurrences off the New England coast. The crew was informed during the mission that support ships off the coast of Maine had located a zone of discolored water near the mouth of the Damariscotta River. This area was observed by the crew, and the DMP later reported:

> Per ground request we just shot a few frames here up through the New England area ending on magazine CX-10 with frame 35. Trying to pick up the red tide around Boothbay, and we did see a lot of red coloration in the water there. However, some of it

looked to me like it was coming out of the river mouths and is really sediment. And I hesitate to term it red tide. We shot some pictures; maybe we can psych it out later.

Examination of the returned photographs suggests that the DMP photographed the area of the Bay of Fundy (fig. 10-11). This area shows the same features that were expected around Boothbay Harbor, mainly discolored reddish water caused by sediments from coastal rivers.

To aid oceanographers in the identification and location of ocean features, the crew was asked to provide the ground-elapsed time (GET) when a target was observed. However, during the postmission debriefings, the crew indicated that time was probably insufficient to identify the exact location of an observed ocean site because they could see such a broad area.

Desert Studies

Deserts occupy nearly one-sixth of the Earth's land masses, but first-order surveys of most desert regions are inadequate. Size, remoteness, and inaccessibility make conventional aerial surveys impractical and costly. Photographs acquired from space, however, can provide reliable data that are useful in the preparation of base maps and in the evaluation of eolian landforms. Orbital images of large areas can be rapidly acquired for the construction of mosaics and for distribution analysis of large-scale phenomena such as color variation and sand dune patterns. As part of the ASTP investigation of deserts and arid lands, visual observations and photography of the following types of features were scheduled.

Feature	Interest
Eolian landforms	Dune shape, size, and distribution Dune patterns and their relation to topography, wind, moisture, and vegetation
Desert color	Color transitions within a homogeneous desert Comparison of equatorial desert color with that of high-latitude deserts
Processes of desertification in the Sahel	Land use Evolution of dune patterns and effect on cultivation

Excellent photographs of deserts in Africa, the Arabian Peninsula, Australia, and Argentina were acquired. Photography over the Sahara is extensive and includes two mapping passes over Algeria, Chad, Libya, and Egypt; a strip of 16-millimeter photography over the western Sahara; and numerous hand-held photographs. This photography will be used in an investigation of eolian geomorphology primarily to evolve a classification scheme for deserts in North Africa. In

addition, a mosaic to be constructed from the mapping photography of Egypt will be used in a study of the Western Desert of Egypt by a team of geologists from Ain Shams University, Cairo.

Synoptic photography and astronaut observations also provided valuable information on desert color. Deserts often contain a significant amount of iron compounds that, because of weathering, oxidize into red-colored ferrous oxides. Photography of color zonation within a desert where the sand is derived from the same source (e.g., fig. 10-12) can be used to determine relative age. The crew used the color wheel to calibrate variations in the color of North African sand seas. During photography of the western Sahara with the 16-millimeter DAC, the DMP made the following observation:

> We discovered a large expanse of fairly homogeneous sand desert. No obvious dune patterns . . . We're now coming to the rocky volcanic hills of the northeast edge of the big sand desert. Some very red sand to the north. In fact, it looks almost like a massive parabolic sand dune, black with red sand behind it. And we're coming up on a large band of very black barren-looking hills with great red areas interspersed between them . . . Okay, and at 119:50, we're coming up into a couple of areas where the dunes are now a little better defined; they look like old domes. They're certainly not stars and they're not linear either. And we get farther into the north, there is a little linear pattern, but it's mostly of dome appearances, very homogeneous.

Excellent photographs of the Simpson Desert in Australia were also obtained (e.g., fig. 10-13). Visual observations were made on several passes over the area, and the crew was able to identify dune patterns and desert color.

> We're going over the Simpson Desert right now. And it's just fantastic. It's got dunes in it, looks like they are very long, and they look like road tracks, there are so many of them - like hundreds of parallel road tracks, it's just plain spectacular. (CMP)

> Yeah, and the long red streaks are matching about color 10, I would say on [the color] wheel and some of those long sand streaks, could have either gone to the 9, between 9 and 10, about like 9A. (ACDR)

In Argentina, the crew photographed a little-known dune field (fig. 10-14) and made visual observations of dune shape and the relation of the dune field to the surrounding topography. The following is an excerpt from the discussion of this occurrence during the postmission crew debriefings.

ACDR Okay, it's right over the edge of the Andes Mountains . . . And you could really see how they were crescents; it looked like occasionally maybe the head of the crescent would wash out, and it would tend to be a linear one with lineations on the side. There are all those other little crescents up on the left. That was the area that you wanted me to look at?

PI Yes, that's the only one that we thought existed. We didn't know that there were two dune fields.

ACDR I'd remembered that there was some type of linear feature. There were two rays. One was on this edge down here, which is nearly linear. But the big thing was those huge crescents; then something else linear caught my eye. I see what it is now, those very minor ones in the center left part of the picture.

Co-I This is a particular variety that I haven't seen anywhere else. I have seen a lot of varieties of this generally crescentic dune pattern, but nothing where you have these linear dunes superimposed right on the crescent and they're oriented in this way. That's totally unlike anything I have ever seen anywhere else, so this really is the prize picture as far as desert dune observations went.

ACDR On that little field up there, it's just the way the boundary was very well defined, as opposed to the other where this kind fades out into like a dry lake bed.

Co-I One of the things that is very obvious is the relationship between the edge of the alluvial fan and the beginning of the dune fields; it's very, very sharp. That's not a very red dune field, is it?

ACDR No, it's not.

Co-I Does it look about like the ones you see in the southwestern United States in terms of color?

DMP I would say so. We had a fairly early morning light.

ACDR I think it's close. We have early morning light there and low Sun angles. It didn't have the redness like the Simpson does or anything like that.

Hydrology

Hydrological investigations included photography of snow cover and drainage patterns as well as visual observations of glaciers, firn lines, and closed water basins. Mapping of snowpack distribution is important in the estimation of the

volume of water reaching drainage systems for use in irrigation and the control of floods. Targets for snow cover photography included the Cascade Mountains in the northwestern United States (fig. 10-15), the Andes Mountains in South America, and the Himalaya Mountains in southern Asia. Coverage of the Cascades and Andes was acquired; however, the Himalayan photography was not successful because of cloud cover.

Visual observations of glaciers and firn lines were also scheduled to test the limits of the eye's resolution. The crew was successful in distinguishing firn lines and remarked that this was a function of both texture and color. The following remarks were made during the postmission debriefings.

CMP The best case, I believe, was in the Alberta-British Columbia area. I very easily saw a firn line on one big glacier up there.

PI How did you make the distinction? Why do you think you were able to see that? Because of color or texture?

CMP Texture and color and even shininess, you might say. Surface texture, I guess.

PI The ice being more gray?

DMP Kind of a gray compared to pure white.

ACDR Yes, it goes from white to gray. And the firn line wasn't just a straight line; it was kind of jagged. It wasn't a clear line.

DMP But I thought I could see texture down below it also, that sort of looked like flow patterns going parallel with the glaciers.

A study was also made of major lakes including Lake Chad, the Great Salt Lake, Lake Eyre, and the Caspian Sea. Lake Chad, once one of Africa's largest lakes, lies in the Sahel region between the savanna land and the sandy desert. To the northeast, it is bounded by fossil dunes; from the south, tropical rivers flow into the lake, bringing sediment and freshwater. The rapid decrease in lake size has been attributed to three factors: the influx of sand from the Sahara, the accumulation of sediments deposited by inflowing rivers from the south, and the evaporation of surface waters.

The possibility that Lake Chad might eventually dry up presents a problem because the southern part of the lake is biologically productive and rich in fish. The ASTP photography will be compared to Skylab data to determine the rate of change in the size of Lake Chad. Many more dunes are now visible within the lake (fig. 10-16).

The ASTP photography of the Great Salt Lake in the United States will also be compared to Skylab imagery. Construction of a railroad causeway in 1956 has essentially divided the lake into two basins. Almost 90 percent of the lake's inflow now enters the southern half, resulting in a rise in water level and a decrease in salinity in that half. Conversely, waters in the northern basin have become oversaturated with salts and minerals. This change in salinity is easily detected from orbit because the presence of different types of algae has given each half a different color. These factors have had a serious effect on both the ecology of the lake region and industrial development.

Meteorology

Meteorological investigations were made in a study of cloud features and tropical storms. Photography of cloud features includes Bénard cells, Kármán vortices, mountain waves (rotor clouds), atmospheric bow waves in the lee of islands, and cumulonimbus buildups. The crew also obtained photography of a developing tropical storm in the Caribbean Sea. The following is an excerpt of real-time observations over the storm:

> It doesn't seem to cover so much area, but it does have a rather swirling "V" appearance. I don't see an eye, but I can see where an eye would be. (CMP)

Photographs and visual observations will help meteorologists develop computer models of hurricanes and tropical storms. Stereophotographs of a dissipating storm were also taken and will be used in making a three-dimensional stereoscopic model of the storm to help decipher its "topography." The stereoscopic model in turn will affect theoretical models of storm development and dissipation. Excellent photography of thunderstorms was also acquired and will be used in studies of severe storm development (fig. 10-17).

Unusual photographs of large-scale intersecting cloud streaks were obtained (fig. 10-18). During postmission debriefings, the crew reported that these features were too large to be contrails and had a wedge-shaped appearance:

DMP We saw an awful lot of contrails over the North Atlantic and it's nothing like that. They just don't get that big.

CMP Contrails were lines; these are wedges practically.

QUERY Remember from Skylab, when they took a picture and they thought it was the hot air coming from a ship going through a very low scattered deck about like that, and there was a plume going right across the apparent trend of the clouds. Do you think that maybe that was this same thing?

CMP It's a possibility, I suppose, but at the time it looked natural.

Environmental Studies

Environmental investigations included photography of sources of atmospheric and water pollution and potential sites for sea farming. The crew recognized and observed several different sources of atmospheric pollutants, both manmade and natural. These sources included volcanic plumes, duststorms in the Sahara and the U.S.S.R., brush fires in Africa, oil fires in the Middle East, ship trails, and contrails. Astronaut observations were useful in determining the extent and geographic locations of these features.

Sources of water pollution include suspended sediments, oil spills, and organic compounds. The occurrence of two types of water pollution was documented with photography of the Orinoco River Delta (fig. 10-7). In addition to sediments, the Orinoco River outflow includes a high concentration of humic compounds that result in the discoloration of the ocean waters for hundreds of kilometers. The ASTP information, combined with real-time ground-truth data collection, will allow a better understanding of this phenomenon and its effect on local fisheries.

In cooperation with the International Maritime Commission, observations of oil slicks in North Atlantic ship routes were planned, but cloud cover and the lack of sunglint prevented the acquisition of data. However, observations were made and photographs were taken of oil slicks in the Mediterranean Sea and the Persian Gulf.

The crew was also asked to observe and photograph several areas designated by Jacques Cousteau as potential sites for "sea farming." Three sites were scheduled in real time and included the Adriatic Sea, the waters south of Cuba, and the Strait of Georgia.

CONCLUSIONS

Preparation and execution of the ASTP Earth Observations and Photography Experiment was a highly rewarding experience. The many hours spent in training the crew, both in flyover exercises and in the classroom, brought significant results that attest to the value of man in space flight. The astronauts are enthusiastic about their contributions, and the participating scientists have a considerable amount of new data to be interpreted and analyzed. This analysis will further our vistas in numerous fields of Earth science.

From the results of this experiment, several conclusions can be drawn in regard to the most tangible scientific results and the role of man in space.

Tangible Scientific Results

Evaluation of the scientific return of ASTP observations of the Earth has just begun. It is difficult, at this stage, to determine the most significant contributions. The following are only examples of what has been learned in the considered fields of Earth science.

Geology.- Although many fault systems were studied from orbit, the observations and photographs of the Levantine Rift zone are most prominent. Three major faults were traced to their northernmost extremities where very little was known about them. These faults appear to branch out in north and northeast directions. Branching appears to start at a pivot point for the counterclockwise rotation of the Arabian crustal subplate relative to the African crustal plate. This indicates that fractures in that zone are not simply the result of a rip-apart motion but a complex rotation of the entire Arabian peninsula. The results of detailed mapping of these faults from the ASTP data will add significant insight into the tectonic regime of the Middle East.

Oceanography.- One of the most significant ASTP findings establishes that ocean features such as eddies and internal waves are more common than previously thought. The ASTP crew also established that viewing direction, as well as Sun angle, is extremely significant in observing internal waves. Viewing conditions will be thoroughly documented to allow better planning and preparation for similar activities in the future.

Deserts.- Perhaps the most significant contribution of the experiment is that the ASTP data will help define (1) relative ages of desert areas based on color and (2) direction of desert growth using sand dune patterns in North Africa. The implications of these results, particularly to the African drought problem, include the ability to distinguish, from photographs, areas of recent desert formation and to establish the directions of desert growth. Also, two new unique patterns of dune morphologies were observed: star dunes atop linear dunes in the Gobi Desert and a fish-scale pattern of dense sand dunes overlain by thin linear dunes in Argentina.

Hydrology.- Snow cover over the Cascade Mountains was photographed on separate days to permit studies of melt patterns. These photographs will also be compared to previous images of the same area to establish trends in snow accumulation and melting for hydrological projects.

Meteorology.- The most significant result in the field of meteorology appears to be the photography of a developing storm northeast of Florida and of a dissipating storm over the Atlantic Ocean. Stereoscopic models of these storms will be studied to improve theoretical models of tropical storm development and dissipation.

Environment.- The outflow of the Orinoco River into the Atlantic Ocean was described, and the observations were documented with photographs. In addition to sediments, the Orinoco River outflow includes an unusually high concentration of humic compounds that result in the discoloration of the ocean waters for hundreds of kilometers. The ASTP information combined with real-time ground-truth data collection will allow a better understanding of this phenomenon.

Role of Man in Space

From the ASTP experience, the following conclusions may be made.

1. Man in space can help design instruments or film to be used on unmanned probes. An example is the use of a color wheel to establish the actual range of visible colors of deserts and oceans.

2. A trained observer is probably essential to the study of features and phenomena characterized by transient visibility. An example is internal waves that are visible only under very restricted conditions.

3. An observer in orbit can make immediate interpretations that significantly contribute to solving the problem under investigation; for example, the explanation of the tectonic setting of the Levantine Rift area.

4. A human observer is essential if the purpose of the study is to explore the unknown. A trained observer will scan an entire region and select targets for photography that will draw attention to the significant aspects.

5. From the information learned about deserts on this mission, it is concluded that much more can yet be attained from orbital surveys in this field. Desert study will also be important in comparative planetological studies; many of the features of Mars are similar to those of the Earth's deserts.

6. Earth observations and photography tasks require a flexible platform where viewing angles and interior lighting conditions can be controlled. The design of instrumentation should allow control of imaging systems by the observer.

7. For the successful performance of Earth observations tasks, the observer must be well prepared and well trained. The exercise must be pursued systematically; otherwise, significant features and phenomena may be overlooked.

REFERENCES

10-1. Earth Photographs From Gemini III, IV, and V. NASA SP-129, 1967.

10-2. Earth Photographs From Gemini VI through XII. NASA SP-171, 1968.

10-3. Cortright, Edgar M., ed.: Exploring Space With a Camera. NASA SP-168, 1968.

10-4. Lowman, Paul D., Jr.: The Third Planet. Weltflugbild. Reinhold A. Muller (Zurich, Switzerland), 1972.

10-5. Musgrove, R. G.: Lunar Photographs From Apollos 8, 10, and 11. NASA SP-246, 1968.

10-6. Kopal, Zdenek: A New Photographic Atlas of the Moon. Taplinger Publishing Co. (New York), 1971.

10-7. El-Baz, Farouk: New Geological Findings in Apollo 15 Lunar Orbital Photography. Proceedings of the Third Lunar Science Conference, vol. 1, MIT Press (Cambridge, Mass.), 1972, pp. 39-61.

10-8. El-Baz, Farouk; and Roosa, S. A.: Significant Results From Apollo 14 Lunar Orbital Photography. Proceedings of the Third Lunar Science Conference, vol. 1, MIT Press (Cambridge, Mass.), 1972, pp. 63-83.

10-9. El-Baz, Farouk; and Worden, A. M.: Visual Observations From Lunar Orbit. Sec. 25, Part A, of the Apollo 15 Preliminary Science Report. NASA SP-289, 1972.

10-10. El-Baz, Farouk; Worden, A. M.; and Brand, V. D.: Astronaut Observations From Lunar Orbit and Their Geologic Significance. Proceedings of the Third Lunar Science Conference, vol. 1, MIT Press (Cambridge, Mass.), 1972, pp. 85-104.

10-11. Mattingly, T. K.; El-Baz, Farouk; and Laidley, Richard A.: Observations and Impressions From Lunar Orbit. Sec. 28 of the Apollo 16 Preliminary Science Report. NASA SP-315, 1972.

10-12. Mattingly, T. K.; and El-Baz, Farouk: Orbital Observations of the Lunar Highlands on Apollo 16 and Their Interpretation. Proceedings of the Fourth Lunar Science Conference, vol. 1, MIT Press (Cambridge, Mass.), 1973, pp. 49-56.

10-13. Evans, R. E.; and El-Baz, Farouk: Geological Observations From Lunar Orbit. Sec. 28 of the Apollo 17 Preliminary Science Report. NASA SP-330, 1974.

10-14. El-Baz, Farouk; and Evans, R. E.: Observations of Mare Serenitatis From Lunar Orbit and Their Interpretation. Proceedings of the Fourth Lunar Science Conference, vol. 1, MIT Press (Cambridge, Mass.), 1973, pp. 139-147.

10-15. Kaltenbach, J. L.; Lenoir, W. B.; McEwen, M. C.; Weitenhagen, R. A.; and Wilmarth, V. R., eds.: Skylab 4 Visual Observations Project Report. NASA TM X-58142, 1974.

10-16. Committee on Colorimetry: The Science of Color. The Optical Society of America (Washington, D.C.), 1963, p. 129.

TABLE 10-I.- EARTH OBSERVATIONS TEAM

Name	Discipline	Affiliation
J. R. Apel	Oceanography	National Oceanic and Atmospheric Administration (NOAA)
J. C. Barnes[a]	Snow mapping	Environmental Research and Technology, Inc.
P. G. Black[a]	Meteorology	NOAA
G. Borstad	Oceanography	Bellairs Research Institute, McGill University, Canada
C. S. Breed[a]	Deserts	Museum of North Arizona and U.S. Geological Survey (USGS)
N. S. Brill	Red tide	Commonwealth of Massachusetts
W. J. Campbell[a]	Hydrology	University of Puget Sound
R. Citron	Short-lived phenomena	Smithsonian Institution
J. Cousteau	Sea farming	Cousteau Society
R. Dietz[a]	Marine geology	NOAA
L. Dunkelman	Atmosphere	University of Arizona and Goddard Space Flight Center (GSFC)
F. El-Baz[b]	General	Smithsonian Institution
G. Ewing	Oceanography	Woods Hole Oceanographic Institute
R. K. Holz	Demography	University of Texas at Austin
W. A. Hovis	Oceanography	GSFC
R. C. Junghans	Environment	NOAA
J. L. Kaltenbach	Skylab results	Lyndon B. Johnson Space Center (JSC)
W. B. Lenoir	Skylab results	JSC
N. H. MacLeod	Deserts and Agriculture	American University
G. A. Maul[a]	Oceanography	NOAA
M. C. McEwen	Skylab results	JSC
E. D. McKee[a]	Deserts	USGS
S. McLafferty	General	Smithsonian Institution
D. A. Mitchell	General	Smithsonian Institution
J. A. Murphy	General	Smithsonian Institution
W. R. Muehlberger[a]	Geology	University of Texas at Austin

[a]Co-Investigator.

[b]Principal Investigator.

TABLE 10-I.- Concluded

Name	Discipline	Affiliation
K. M. Nagler	Weather patterns	NOAA
D. K. Odell	Oceanography	University of Miami
D. M. Pirie	Oceanography	Army Corps of Engineers, California
P. R. Pisharoty[a]	Hydrology	Indian Space Research Organization (ISRO), India
D. E. Pitts	Color Science	University of Houston
R. O. Ramseier	Hydrology	Department of the Environment, Canada
J. W. Sherman	Meteorology	NOAA
L. T. Silver[a]	Geology	California Institute of Technology
R. E. Stevenson[a]	Oceanography	Scripps Institute of Oceanography
F. M. Suliman	Deserts	College of Education, Qatar
G. A. Swann	Geology	USGS
V. R. Wilmarth	Skylab results	JSC
R. Wolfe	General	Smithsonian Institution
S. P. Vonder Haar	Oceanography	University of Southern California
C. Yentsch[a]	Red tide	Bigelow Laboratory, Maine
M. Youssef	Deserts	Ain Shams University, Egypt

[a]Co-Investigator.

TABLE 10-II.- PHOTOGRAPHIC MAPPING SITES

Site	Name	Objective
M1	Gulf Stream	The Gulf Loop Current and the Gulf Stream from eastern Florida to its confluence with the Labrador Current
M2	New Zealand	The Alpine Fault in South Island and the coastal waters between the two islands and north of North Island
M3	Southern California	Coastal waters off California, the San Andreas Fault system, and the Mohave Desert
M4	Himalaya Mountains	Ocean features in the Indian Ocean and Arabian Sea, the flood plain of the Indus River, drainage patterns, and snow cover in the Himalayas
M5	Arabian Desert	The Afar Triangle, dune patterns in Ar-Rub Al-Khali, and coastal processes at Doha, Qatar
M6	Australia	Dune patterns and erosional features in the Simpson Desert, the Great Barrier Reef, and eddies in the Coral Sea
M7	African drought	Vegetation and land use patterns in the Sahel, desert colors in northeastern Africa, the Nile River Delta, and the Levantine Rift
M8	Falkland Current	The Falkland Current and its confluence with the Brazil Current east of South America
M9	Sahara	Vegetation and land use patterns in the Sahel, desert colors and dune patterns in the Sahara, and the coastal waters off Tripoli
M10	Northern California	Coastal waters off northern California and subsystems of the San Andreas Fault
M11	New England	Eddies and gyres in the Gulf of Mexico, the Mississippi River Delta, Chesapeake Bay, and coastal waters off New England

TABLE 10-III.- VISUAL OBSERVATION TARGETS

Site no.	Target
1	New Zealand
2	Southwestern United States
	2A Southern California
	2B Baja California
	2C California Current
	2D Great Salt Lake
	2E Guadalajara
3	Weather Belt
	3A Cloud features
	3B Tropical storms
	3C Hawaii
	3D Kuroshio Current
4	Northern North America
	4A Snow peaks
	4B Puget Sound
	4C Superior iron
	4D Sudbury nickel
5	Eastern North America
	5A Gulf of Mexico
	5B Gulf Stream
	5C Labrador Current
	5D Central American structures
	5E Florida red tide
	5F New England red tide
	5G Chesapeake Bay
6	Northern Atlantic
	6A Oil slicks
	6B London
7	Northern South America
	7A Humboldt Current
	7B Nazca Plain
	7C Internal waves
	7D Peruvian desert
	7E Orinoco River Delta
	7F Galapagos Islands
	7G Caribbean Sea
8	Southern South America
	8A Falkland Current
	8B Chilean Andes
	8C Dune field
	8D Paraná River
	8E Circular structures
9	Africa and Europe
	9A Afar Triangle
	9B Arabian Peninsula
	9C Guinea Current
	9D Desert colors
	9E Oweinat Mountain
	9F Nile Delta
	9G Levantine Rift
	9H Niger River Delta
	9I Algerian Desert
	9J Tripoli
	9K Strait of Gibraltar
	9L Alps
	9M Danube Delta
	9N Anatolian Fault
	9O Volcanics
	9P Bioluminescence
10	Africa and India
	10A Great Dike
	10B Somali Current
	10C Arabian Sea
	10D Himalaya Mountains
	10E Takla Makan Desert
11	Australia
	11A Playas
	11B Coral Sea
	11C Simpson Desert
	11D ANZUS Eddy
12	Antarctican ice
	12A Icebergs

TABLE 10-IV.- CLASSROOM TRAINING

Date	Subject	Lecturer
Aug. 5, 1974	Plan for Earth observations and photography	F. El-Baz
Aug. 16	Global tectonics and astroblemes	R. Dietz
Oct. 10	Background, terminology, and Skylab 4 results (oceanography)	S. P. Vonder Haar
Oct. 18	Snow and ice	J. C. Barnes, W. J. Campbell, and R. O. Ramseier
Nov. 6	Southwest U.S. tectonics Site selection procedures	L. T. Silver F. El-Baz
Nov. 15	Ocean currents and eddies Sites for observation	G. A. Maul R. E. Stevenson and G. Ewing
Dec. 3	African rift system and Central America	W. R. Muehlberger
Dec. 20	Deserts and sand dune patterns	E. D. McKee and C. S. Breed
Jan. 7, 1975	Cloud features and tropical storms	P. G. Black
Jan. 31	Groundtracks and sites	F. El-Baz
Mar. 5	Onboard site book	F. El-Baz
Mar. 18	Visual observation sites	F. El-Baz
Mar. 19	Ocean observation tasks	Oceanography Team
Apr. 1	Groundtracks and sites	F. El-Baz
Apr. 9	Groundtracks and sites	F. El-Baz
May 20	Review of observation tasks	F. El-Baz
June 2	Review of observation tasks	F. El-Baz
June 20	Review of observation tasks	F. El-Baz
July 8	Review of observation tasks	F. El-Baz
July 13	Review of observation tasks	F. El-Baz

TABLE 10-V.- FLYOVER EXERCISES

Flyover	Observation targets
Houston to Los Angeles	Texas coastal plain Karst topography Basin and range topography Volcanic features Sonora and Mohave Deserts (site 2A) San Andreas Fault system (site 2A)
California	San Andreas Fault (site 2A) Garlock Fault (site 2A) Desert varnished hills (site 2A) Sand dunes in the Algodones Desert Ocean features in waters off California (site 2A)
Gulf Coast	Coastal sediments Mississippi River Delta Gulf Loop Current (site 5A) Red tide off the western coast of Florida (site 5E)
Florida	Gulf Stream (site 5B) Red tide (site 5E)
East Coast	Gulf Stream (site 5B) Sediment and pollution in Chesapeake Bay (site 5G) Internal waves Sand dunes on Cape Cod Red tide off Massachusetts and Maine (site 5F)
Southwestern United States	Dune patterns at White Sands and Great Sand Dunes National Monuments Circular structures in the San Juan Mountains Copper mines
Northwestern United States	Fault systems in northern California (site 2C) Metamorphic foothills of the Sierra Nevadas (site 2C) Snow-covered peaks in Washington (site 4A) Blue Glacier and Southern Cascades Glacier Sediments in Puget Sound

TABLE 10-VI.- MUNSELL COLOR DESIGNATIONS[a]

OF THE ASTP COLOR WHEEL

Color wheel no.	Desert colors[b]		Color wheel no.	Ocean colors[c]	
	A	B		A	B
1	2.5R 6/6	2.5R 7/8	28	10BG 4/4	10BG 5/6
2	2.5R 5/8	2.5R 6/10	29	10BG 5/4	10BG 6/6
3	5R 4/10	5R 5/12	30	10BG 6/4	10BG 7/6
4	5R 5/8	5R 6/10	31	2.5B 6/6	2.5B 7/8
5	5R 6/6	5R 7/8	32	2.5B 5/6	2.5B 6/8
6	7.5R 6/6	7.5R 6/8	33	2.5B 4/6	2.5B 5/8
7	7.5R 5/8	7.5R 6/10	34	5B 4/4	5B 5/6
8	7.5R 4/10	7.5R 5/12	35	5B 5/4	5B 6/6
9	10R 4/8	10R 5/10	36	5B 6/4	5B 7/6
10	10R 5/6	10R 6/8	37	7.5B 6/6	7.5B 7/8
11	10R 6/4	10R 7/6	38	7.5B 5/6	7.5B 6/8
12	2.5YR 7/6	2.5YR 8/8	39	7.5B 4/6	7.5B 5/8
13	2.5YR 6/8	2.5YR 7/10	40	10B 4/8	10B 5/10
14	2.5YR 6/10	2.5YR 6/12	41	10B 5/6	10B 5/8
15	5YR 5/8	5YR 6/10	42	10B 6/6	10B 6/8
16	5YR 6/6	5YR 7/8	43	2.5PB 5/6	2.5PB 6/8
17	7.5YR 6/6	7.5YR 7/8	44	2.5PB 4/6	2.5PB 5/8
18	7.5YR 5/8	7.5YR 6/10	45	2.5PB 3/6	2.5PB 4/8
19	10YR 5/6	10YR 6/10	46	5PB 3/8	5PB 4/10
20	10YR 6/6	10YR 7/8	47	5PB 4/8	5PB 5/10
21	10YR 7/4	10YR 8/6	48	5PB 5/6	5PB 6/8
22	2.5Y 8/6	2.5Y 8.5/6	49	7.5PB 5/8	7.5PB 6/10
23	2.5Y 8/4	2.5Y 7/4	50	7.5PB 4/10	7.5PB 5/12
24	7.5YR 8/4	7.5YR 7/4	51	7.5PB 3/10	7.5PB 4/12
25	2.5YR 8/4	2.5YR 7/4	52	5P 2.5/4	5P 3/10
26	7.5R 8/4	7.5R 7/4	53	5RP 2.5/4	5RP 3/6
27	2.5R 8/4	2.5R 7/4	54	5R 2.5/4	5R 3/4

[a]Each designation indicates hue, value, and chroma in the form H V/C. Hue is divided into 10 groups (red, yellow-red, yellow, green-yellow, green, blue-green, blue, purple-blue, purple, and red-purple); each group is further subdivided by use of numerals (2.5, 5, 7.5, and 10 for the ASTP color wheel). Value is specified on a numerical scale from 1 (black) to 10 (white). Chroma is indicated numerically from 0 to 12 (for the ASTP color wheel).

[b]See fig. 10-2(a).

[c]See fig. 10-2(b).

TABLE 10-VII.- MISSION TASK ASSIGNMENTS

Revolution	Mapping tasks		Visual observation tasks	
	Site	Crewmember (a)	Site	Crewmember (a)
15	M1	ACDR	5A, 5B, 5C	DMP
17	M2, M3	DMP	12A, 1, 3A, 2A, 4C, 5C	CMP
39	M4	DMP	10A, 10B, 10C, 10D, 10E	DMP
40	M5	DMP	9A, 9B	DMP
42			8A, 3A, 9H, 9I, 9J	DMP
45			5D, 5A, 5E, 5F, 5C	DMP
46			2E, 4D	CMP
64	M6	ACDR	11C, 11B, 3A	CMP
71	M7	DMP	9C, 9D, 9E, 9F, 9G	CMP
72	M8, M9	ACDR	12, 8A, [b]9H, [b]9I, [b]9J	DMP
73			3A, 9K, 9L	ACDR
74			7B, 7C, 6A, 6B	ACDR
78			3C, 4A	DMP
79			11A, 11B, 3A	DMP
88			8B, 8C, 8D, 8E, 3A, 9K, 9L	ACDR
90			5D, 5A, 5E, 5G, 5F, 5C, 6A, 9P	DMP
104			7A, 7D, 7E	ACDR
106			3B, 2B, 2E, 4D	CMP
107	M10	CMP	2C, 2D	CMP
108			3C, 4B	CMP
123			11D	DMP
124			4A, 4C, 4D	CMP
134			7F, 7G, 6A, 6B, 9M, 9N, 9P	ACDR
135	M11	DMP	3B, 5A, 5G, 5F, 6A, 9L, 9O, 9P	CMP

[a]ACDR, Apollo commander; DMP, docking module pilot; CMP, command module pilot.
[b]DAC.

TABLE 10-VIII.- AIRCRAFT SUPPORT SENSOR DATA

Sensor type	Lens focal length, cm (in.)	Film type	Filtration	Spectral band, nm	Percent of overlap
Vinten	4.45 (1.75)	Panatomic-X, 3400	Schott GG 475 and Schott BG 18	475 to 575	60
Vinten	4.45 (1.75)	Panatomic-X, 3400	Schott OG 570 and Schott BG 38	580 to 680	60
Vinten	4.45 (1.75)	Infrared Aerographic, 2424	Schott RG 645 and Corning 9830	690 to 760	60
Vinten	4.45 (1.75)	Aerochrome Infrared, 2443	Wratten 12	510 to 900	60
RC-10	15.24 (6)	Aerial color, SO-242	2.2AV	400 to 700	60

TABLE 10-IX.- PHOTOGRAPHIC MAPPING RESULTS

Mapping pass	Description	Remarks
M1 Gulf Stream	Fracture pattern of a micro-crustal plate that includes the Yucatán Peninsula Eddies and currents in the Yucatan Channel Red tide off western coast of Florida Eddies and gyres of Gulf Stream	Mapping camera photography was canceled on revolution 15/16 because of Flight Plan problems.
M2 New Zealand	Photography of Alpine Fault Internal waves Plankton blooms Eddies in South Pacific	Alpine Fault photography was not successful because of cloud cover; however, all other objectives were achieved.
M3 Southern California	Ocean water color Red tide off coast of California Subsystems of San Andreas Fault Desert colors and processes in the Mohave Desert	The ocean part of the mapping strip was partly cloudy; excellent photography was obtained of the land part.

TABLE 10-IX.- Continued

Mapping pass	Description	Remarks
M4 Himalaya Mountains	Shoreline processes at Zambezi River Delta margin Sediment plumes in Somali Current Ocean currents in Arabian Sea Flood plains of the Indus River Drainage patterns of foothills of Himalayas Photography of snow cover	Excellent photography was acquired over the Indian Ocean and Arabian Sea; however, most of India (and particularly the Himalayas) was completely cloud covered.
M5 Arabian Desert	Afar Triangle Structures on border of Red Sea rift Dune patterns in Ar-Rub Al-Khali Coastal processes at Doha, Qatar	Scattered clouds covered the western part of the Afar Triangle, but the weather was clear from eastern Afar to Qatar and good photography was acquired.
M6 Australia	Playas in the Lake Eyre region Dune patterns in Simpson Desert Great Barrier Reef Eddies in the Coral Sea	The weather was good all along the revolution 64 groundtrack, and excellent photographs of Australia and the Coral Sea were obtained.

TABLE-10-IX.- Continued

Mapping pass	Description	Remarks
M7 African drought	Guinea Current Lake Chad region, vegetation and land use patterns Desert colors in northeastern Africa Sand dune patterns and their relation to vegetation and wind Nile River Delta Levantine Rift: structures of Golan Heights and southern Turkey	Photography of the Guinea Current was not successful because of cloud cover; however, the weather was clear from Lake Chad to the Levantine Rift and excellent photographs were obtained.
M8 Falkland Current	Continental-shelf waters Falkland Current and its relationship to fisheries	The spacecraft attitude for this pass was not nominal and resulted in oblique photography with the horizon occupying much of the frames.
M9 Sahara	Niger River Delta: dune patterns and land use of the Inland Delta for comparison with Skylab data on the Sahel Desert color and relation to age Desert dunes and their relation to topography, moisture, and vegetation Coastal processes at Tripoli Eddies in waters between Tripoli and Sicily	South of the Niger River Delta, cloud cover obscured much of the terrain, but the weather was clear north of the delta. Photographs of the Sahara are slightly overexposed, but those over the land-water interface at Tripoli are excellent.

TABLE 10-IX.- Concluded

Mapping pass	Description	Remarks
M10 Northern California	Ocean water color Red tide occurrences Subsystems of San Andreas Fault Metamorphic foothills of Sierra Nevadas	Photographs of northern California are good, although some frames are slightly over-exposed.
M11 New England	Mexican volcanoes Sediment patterns in Gulf of Mexico waters Eddies and gyres in Gulf of Mexico Mississippi River Delta Potomac River pollution Red tide occurrences off coast of Massachusetts and Maine	Mapping pass photography on revolution 135/136 is out of focus, probably because the 80-mm lens (used for the electrophoresis experiment) was substituted for the 60-mm lens.

TABLE 10-X.- VISUAL OBSERVATION RESULTS

Target designation		Description	Remarks
1	New Zealand	Alpine Fault photographs Internal waves between North and South Islands Plankton blooms Pacific water color	The Alpine Fault was cloud covered, but visual observations of ocean waters northeast of New Zealand were recorded. The color wheel was used, and the crew reported that the ocean color was close to 47-B.
2A	Southern California	Current boundaries Red tide off coast Gran Desierto color Desert varnished hills	Cloud cover obscured much of the ocean, but interesting cloud waves were observed in the lee of the Channel Islands. A color wheel reading of 16-A was given to the Gran Desierto.
2B	Baja California	Pacific water color Bahía Concepción Fault Internal waves in Gulf of California Gray rock exposures	Oblique photographs were obtained over the Baja peninsula, but there were no crew comments.
2C	California Current	Pacific water color Faults west of San Andreas Foothill metamorphic range	There was some cloud cover over the ocean, but a color reading of 47-B was taken for the coastal waters just offshore from San Francisco.

TABLE 10-X.- Continued

Target designation		Description	Remarks
2D	Great Salt Lake	Bonneville track Color boundaries and sediment plumes in lake Bingham copper mine Snow cover on the Wasatch Range	Excellent photographs of the Great Salt Lake were acquired. In addition, the crew reported that the Bonneville track could be easily detected.
2E	Guadalajara	Major fault lines Big Bend structures	No visual observations were made or photographs taken of the Guadalajara area; however, good photography was obtained of a part of the Mexican volcanic belt southeast of Guadalajara.
3A	Cloud features	Photographs of convective clouds	A number of excellent photographs were obtained including Benard cells, atmospheric bow waves, rotor clouds, and severe thunderstorms.
3B	Tropical storms	Storm centers Texture of storms	Good data were acquired on both developing and dissipating tropical storms.
3C	Hawaii	Upwellings, bow waves, island wakes Kilauea Volcano	No photographs were taken of the Hawaiian islands, but excellent data were obtained of eddies and currents southeast of the islands.
3D	Kuroshio Current	Ocean current boundary Plankton blooms	Some photography was acquired in the South China Sea.
4A	Snow cover	Snow-peaked mountains Glaciers and firn lines	Excellent photographs were obtained of glaciers and snow-peaked mountains in both the Cascade and Canadian Rocky Mountains.

TABLE 10-X.- Continued

Target designation		Description	Remarks
4B	Puget Sound	Suspended sediments Gyres Glaciers and firn lines	Valuable photographic and verbal data were obtained of sediments and gyres in the Puget Sound.
4C	Superior iron	Color oxidation zones	No photographs were taken but visual observation comments were made on color oxidation zones in the Superior region.
4D	Sudbury nickel	Color oxidation zones	Photography of the Sudbury area was unsuccessful because of cloud cover.
5A	Gulf of Mexico	Eddies in Yucatan Channel Florida Current Gulf Loop Current Internal waves in Gulf	Excellent data were obtained, including photography of eddies in the Yucatan Channel and current boundaries in the Gulf of Mexico.
5B	Gulf Stream	Ocean current boundary Internal waves Confluence with Labrador extension	This target was canceled on revolution 15/16 because of Flight Plan problems.
5C	Labrador Current	Ocean current boundary Confluence with Gulf Stream	The ocean northeast of Newfoundland was cloud covered and no photographs were taken.
5D	Central American structures	Bartlett Fault extension Graben valley structures	Central America was usually cloud covered and visual observations of fault structures could not be made.

TABLE 10-X.- Continued

Target designation		Description	Remarks
5E	Florida red tide	Red tide location Color and shape of bloom	The crew reported cloud cover over the Florida peninsula during every visual observation pass.
5F	New England red tide	Red tide location Color and shape of bloom	Boothbay Harbor in Maine was always cloud covered, but excellent photographs of coastal waters of Massachusetts and Canada were taken.
5G	Chesapeake Bay	Sediment gyres Pollution in Potomac River	Valuable photographic and verbal data were obtained of sediment gyres and pollution plumes in the Chesapeake Bay.
6A	Oil slicks	Oil slick extent Color and location	No oil slicks were observed in the North Atlantic, but some photographs of slicks were acquired over the Persian Gulf and the Mediterranean Sea.
6B	London	Sediments and boundaries in English Channel London Harbor area	England was usually cloud covered, but some photographs were taken along the coasts of England and France.
7A	Humboldt Current	Ocean current boundary Gyres in water	Photography of the Humboldt Current was successful.
7B	Nazca Plain	Nazca Plain markings Peruvian desert landforms	Some photography was obtained of the Nazca region, but the crew could not definitely confirm visual sightings of the Nazca Plain markings.
7C	Internal waves	Photographs of internal waves	Excellent photographs were taken of internal waves off Thailand and west of Spain.
7D	Peruvian desert	Dune fields Nazca Plain markings	Valuable photographic data of dune fields in the Peruvian desert were acquired.

TABLE 10-X.- Continued

Target designation	Description	Remarks
7E Orinoco River Delta	Photographs of delta Water color near Barbados	Photographic and verbal data of the Orinoco River Delta included excellent photography of ocean waters between the delta and Barbados as well as visual observations of the extent of "brown water" outflow from the delta.
7F Galapagos Islands	Upwellings Bow waves Island wakes Internal waves	Excellent photography was acquired of the volcanic calderas on the Galapagos and of the complex atmospheric wave patterns surrounding the islands.
7G Caribbean Sea	Eddies Gulf Stream	A number of photographs were taken of the Caribbean waters and the islands of Cuba and Jamaica.
8A Falkland Current	Ocean current boundary Plankton blooms Confluence with Brazil Current	The spacecraft attitude was not nominal for the revolution 72 pass, and the viewing angle out window 3 was very oblique.
8B Chilean Andes	Color oxidation Structures and lineaments	The Chilean Andes were cloud covered and only a few very high peaks were visible.
8C Dune field	Dune field color Dune pattern and orientation Relation with topography	Excellent photography was obtained of this little-known dune field and of a smaller unknown field to the east.

TABLE 10-X.- Continued

Target designation	Description	Remarks
8D Paraná River	Photographs of dam sites	The weather over Paraguay and Brazil was amazingly clear, and excellent data were acquired of potential dam sites on the Paraná and Paraguay Rivers. Additional photographs were taken of the Amazon River.
8E Circular structures	Photographs of two structures	Excellent photography of one possible astrobleme was obtained.
9A Afar Triangle	Ethiopian Plateau scarp Red Sea mountains	The Afar Triangle was mostly cloud covered. The infrared photography is out of focus.
9B Arabian Peninsula	Structures normal to Red Sea Desert color Dune types Coastline of Qatar	Infrared photography of the Arabian Peninsula is out of focus.
9C Guinea Current	Ocean current boundary Gyres in water	Currents and gyres in the Gulf of Guinea could not be observed because of cloud cover.
9D Desert colors	N'Djamena photographs Desert colors Dune patterns	Excellent photography was obtained of the Lake Chad area and of desert colors and dune patterns in the Libyan Desert.
9E Oweinat Mountain	Photographs of mountain Structures in mountain Color oxidation zones	Valuable data were obtained over the Oweinat Mountain, including excellent photography and verbal observations of structural features and color zonations.

TABLE 10-X.- Continued

Target designation		Description	Remarks
9F	Nile Delta	Observation of pyramids Photographs of Cairo Gulf of Suez structures	A number of photographs were acquired over the Nile Delta and included excellent near-vertical photography of the Cairo area.
9G	Levantine Rift	Arcuate fault photographs Terminations of faults	Excellent data were obtained on the arcuate terminations of the Levantine Rift.
9H	Niger River Delta	Dune generations Vegetation patterns	Photography of the Niger River Delta was not successful because of cloud cover.
9I	Algerian Desert	Desert colors Dune patterns Interdune areas Desert and vegetation relationship	Good photography was taken of the Algerian Desert; observations of color zones and sandstorms were also made.
9J	Tripoli	African coastline Eddies, gyres, current boundaries, internal waves in Mediterranean Sea	Data for this target included good photography of the land-water interface at Tripoli and of current boundaries in the Mediterranean Sea.
9K	Strait of Gibraltar	Coastline at Casablanca Atlas Mountains Ocean current boundaries Internal waves	Excellent photography of the Strait of Gibraltar was acquired, and the crew was successful in observing internal waves and current boundaries. Good photographic data were also acquired of central and southern Spain.

TABLE 10-X.- Continued

Target designation	Description	Remarks
9L Alps	Snow cover Glaciers and firn lines	Photographs of snow cover on the Alps were not obtained because of cloud cover.
9M Danube Delta	Photographs of delta Sediment plumes in Black Sea	The crew was successful in photographing the Danube Delta but reported that most of the area was very hazy.
9N Anatolian Fault	Photographs of fault Snow cover on mountains	Good low-Sun-angle photography was acquired of fault zones in Turkey, including excellent data east of Lice (epicenter of the recent earthquake).
9O Volcanics	Photographs of Vesuvius Dark-colored volcanic rocks	Excellent infrared photographs were taken of igneous terrain in Italy.
9P Bioluminescence	Brightening of tracks or zones in the Red Sea, Persian Gulf, and Arabian Sea that may be due to biological factors (nighttime observation)	The crew was not successful in observing bioluminescence in the Red Sea and remarked that they were still in sunglint. However, that was 2 min before the scheduled observation and they were still over the Mediterranean Sea. Earlier in the mission, the mission clocks had been updated 2 min, and the crew was probably using the old ground-elapsed time (GET).
10A Great Dike	Color of Great Dike and surrounding rock	Photography and visual observations of this target were not successful.
10B Somali Current	Zambezi River Delta Coastal sediment plumes Current boundaries Internal waves	Infrared photography of the delta was out of focus, but observations were made of sediment plumes and gyres along the coast.

TABLE 10-X.- Continued

Target designation	Description	Remarks
10C Arabian Sea	Ocean current boundaries	The crew was successful in observing a current boundary, but farther north, high cirrus clouds obscured much of the Arabian Sea.
10D Himalaya Mountains	Photographs of northwestern India	The Himalayas were cloud covered and photographs were out of focus.
10E Takla Makan Desert	Desert colors Dune patterns	The infrared photography of the Takla Makan was out of focus, but observations were made of what was probably a sandstorm over the desert.
11A Playas	Lake Eyre deposits Desert erosion and dune patterns Great Dividing Range	Excellent data were acquired of playas in the Lake Eyre region and included an unusual photograph of the normally dry Lake Eyre with much water.
11B Coral Sea	Coastal sediment plumes Great Barrier Reef Water eddies	Valuable photography was obtained of ocean features in the Coral Sea, and the crew was very successful in locating and describing eddies. They also observed the Great Barrier Reef and remarked that coastal sediments did not extend as far as the reef.
11C Simpson Desert	Desert colors Dune fields Dune types	Excellent photography was obtained that clearly illustrates the characteristic linear dune patterns and the red color of the Simpson Desert.

TABLE 10-X.- Concluded

Target designation	Description	Remarks
11D ANZUS Eddy (Tasmanian Sea)	ANZUS Eddy	Most of the area was cloud covered, but the crew did observe several eddies, one of which may have been the ANZUS Eddy.
12A Icebergs	Photographs of bergs Berg rotation Edge of Antarctica	No icebergs were observed in the Southern Hemisphere; however, the crew did see several large bergs in the North Atlantic and attempted to photograph them.

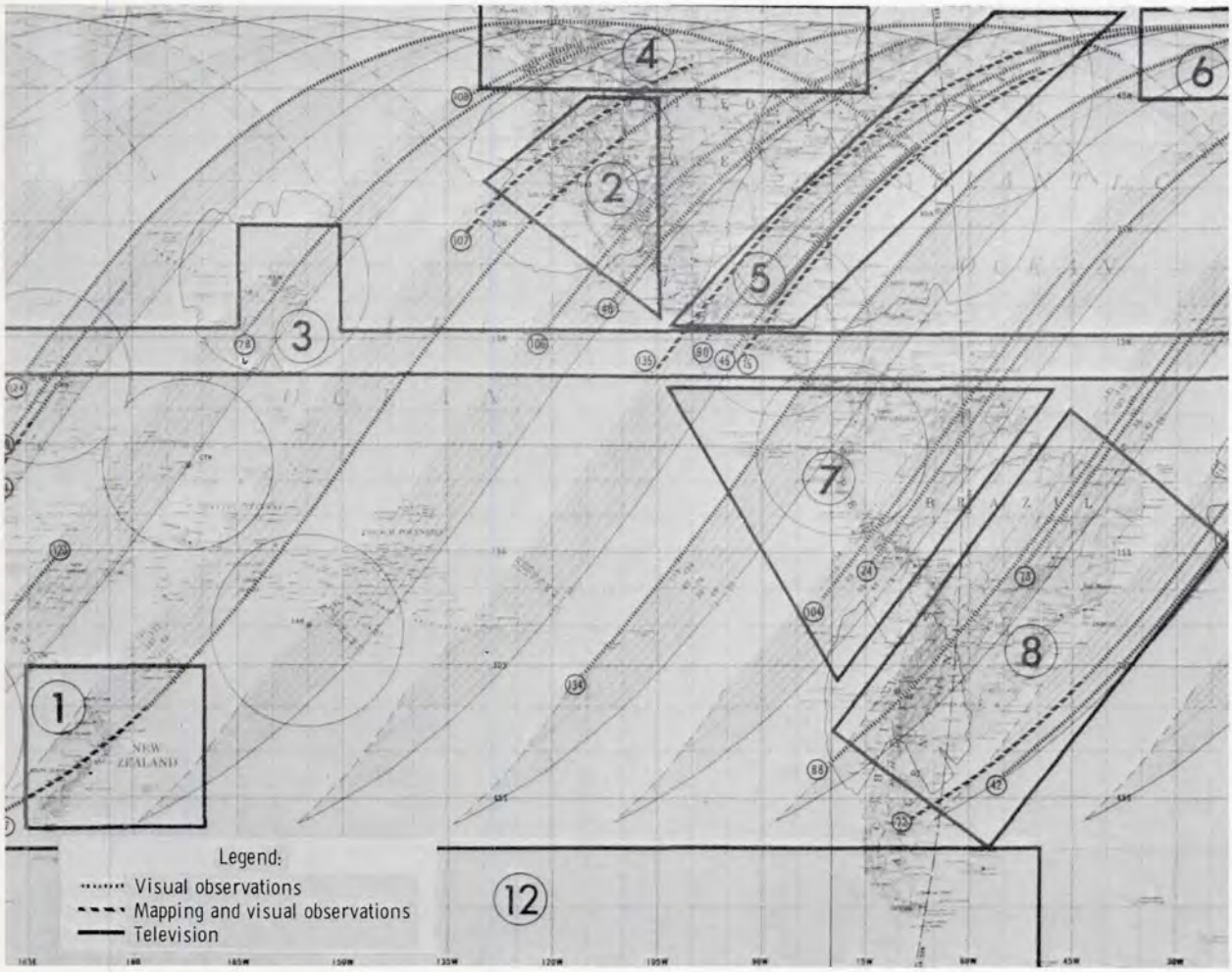

(a) Western Hemisphere.

Figure 10-1.- Maps showing the broad locations of the Earth observation sites. Small circled numbers represent revolution groundtracks for photographic mapping and visual observation tasks; large circled numbers represent the Earth observation sites.

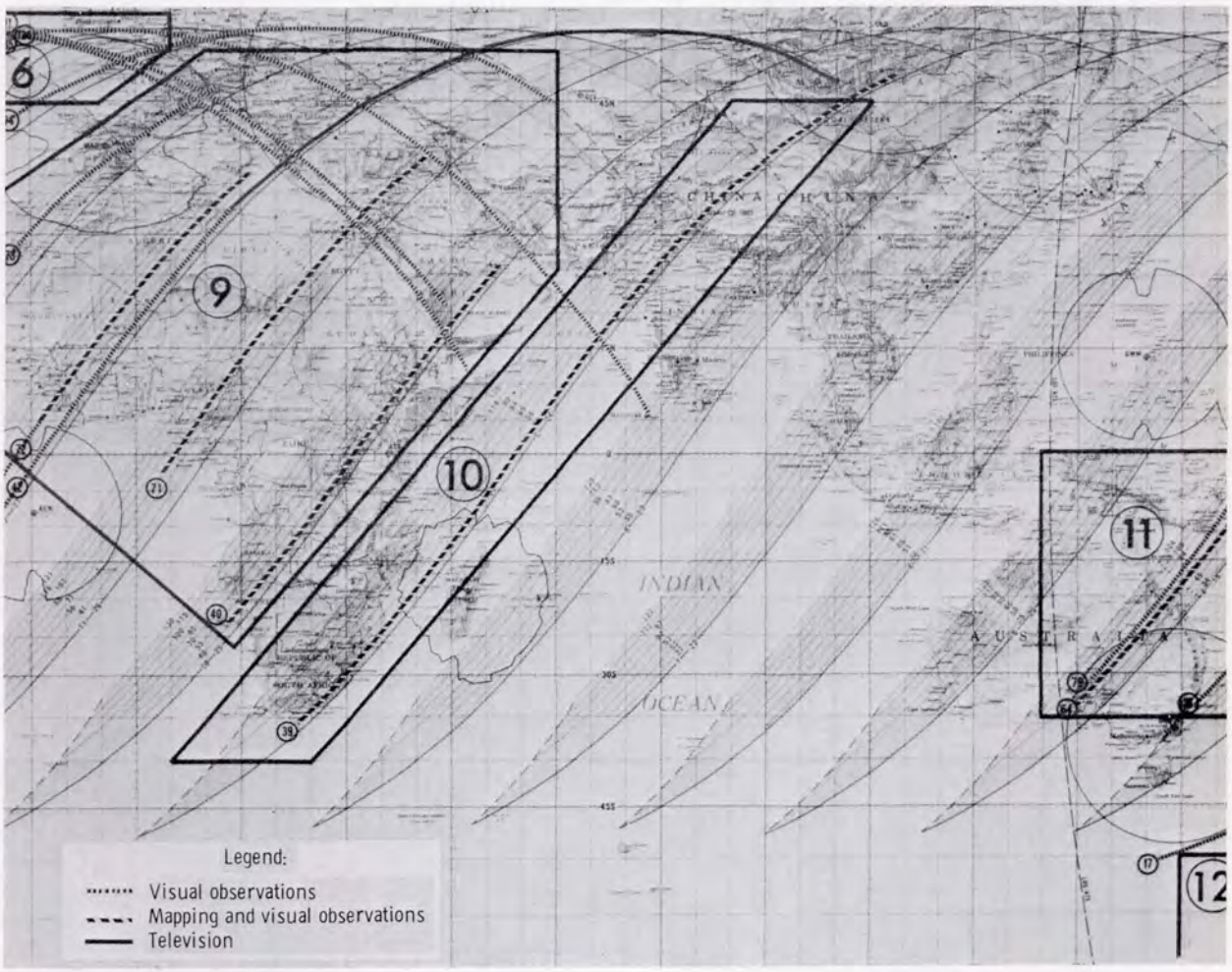

(b) Eastern Hemisphere.

Figure 10-1.- Concluded.

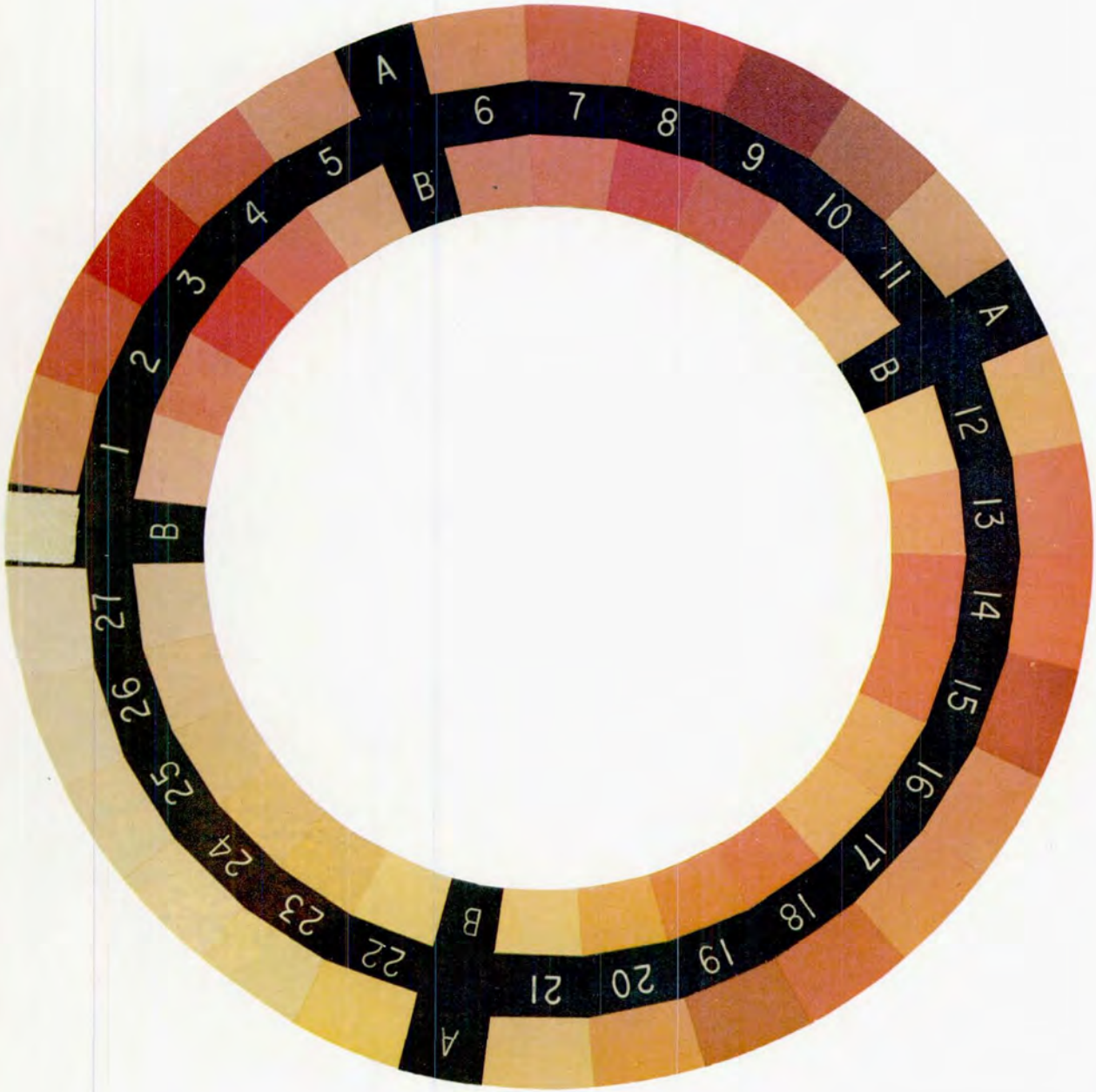

(a) Desert colors.

Figure 10-2.- Color wheel used for assigning desert and ocean colors during the ASTP visual observations. The color chips are from the Munsell color system (see table 10-VI), and their grouping resulted from testing during flyover exercises.

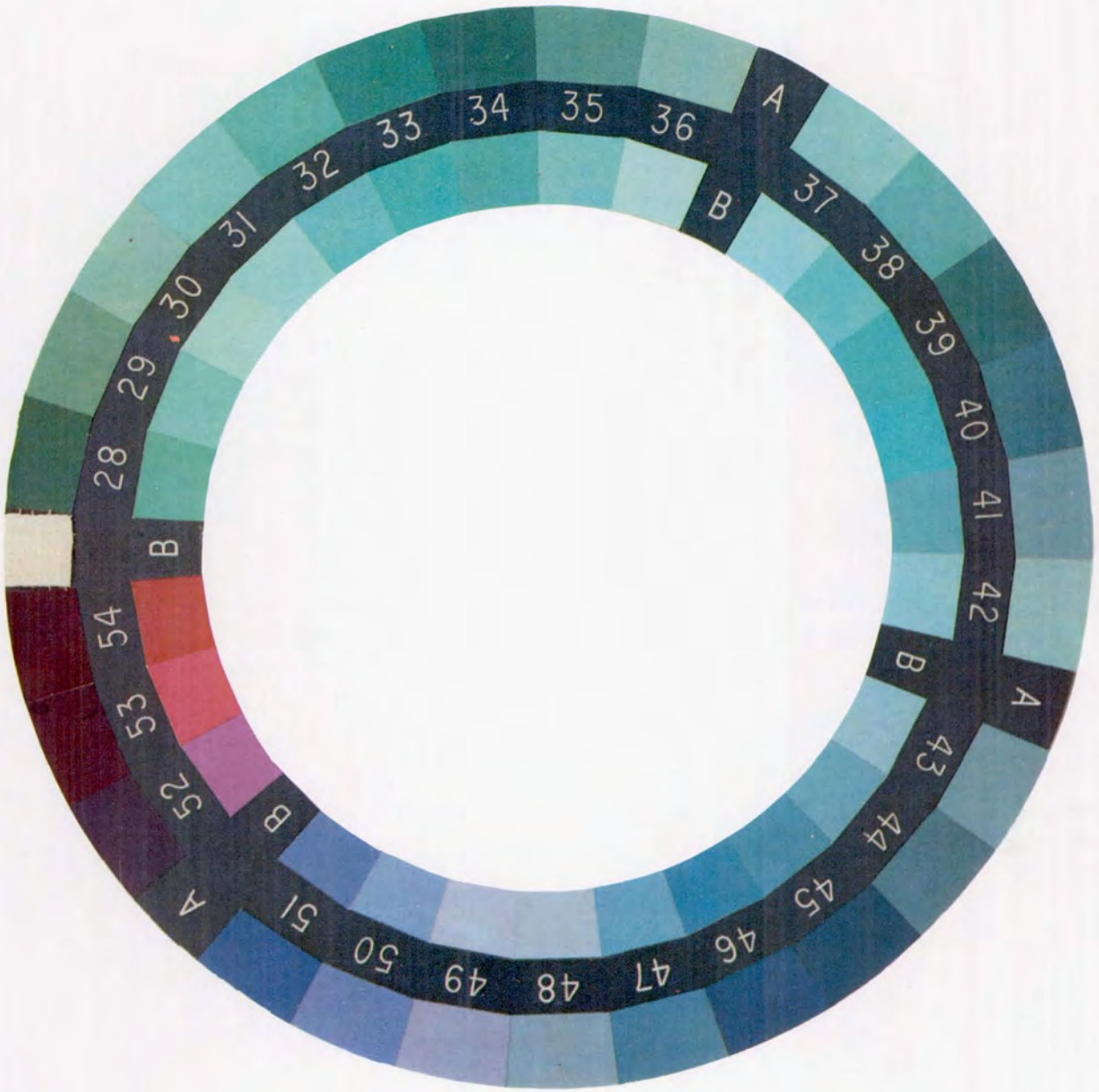

(b) Ocean colors.

Figure 10-2.- Concluded.

Figure 10-3.- World map illustrating locations of support efforts of the ASTP Earth Observations and Photography Experiment.

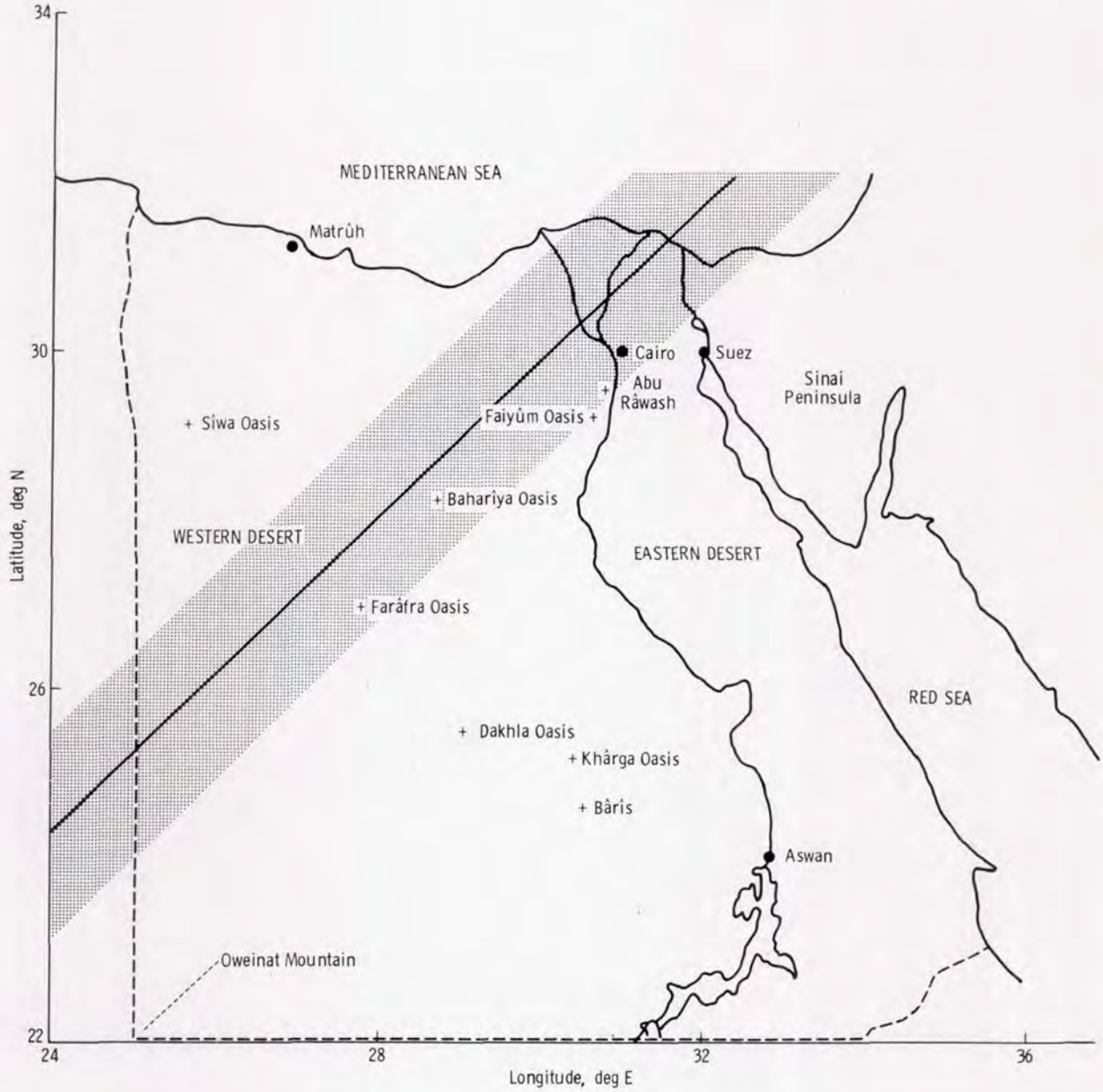

Figure 10-4.- Sketch map of Egypt showing the extent of photographic coverage (dotted area) by the mapping camera on revolution 71 (solid line). A support team from the Ain Shams University in Cairo will provide ground-truth data from the Oweinat Mountain area; the Farâfra, Bahariya, and Faiyûm Oases; and the Abu Râwash region.

Figure 10-5.- The southern part of the Levantine Rift, extending from the Dead Sea to the Sea of Galilee, is distinguished by the linearity of the Jordan River Valley (arrow). To the north, a "fan shaped" complex system of arcuate faults characterizes the rift. One prominent fault parallels the Syrian coast and then makes a noticeable bend to the northwest (AST-9-564).

LEVANTINE RIFT

71

1. OBTAIN 3 STEREO PHOTOGRAPHS OF THE ARCUATE TERMINATIONS OF THE LEVANTINE RIFT.
2. CAN YOU DISTINGUISH RELATED GROUPS OF FAULTS?
3. WHERE IS THE NORTHERNMOST TERMINATION OF THIS FAULT COMPLEX?

REV 71: CM3/SILVER/250/CX12(f8,1/500) 3FR,[RECORD LAST FR NO: PAGE 4]

Figure 10-6.- One page from the Earth Observations Book (visual observation target 9G) that was used by the crew to visually study the Levantine Rift area.

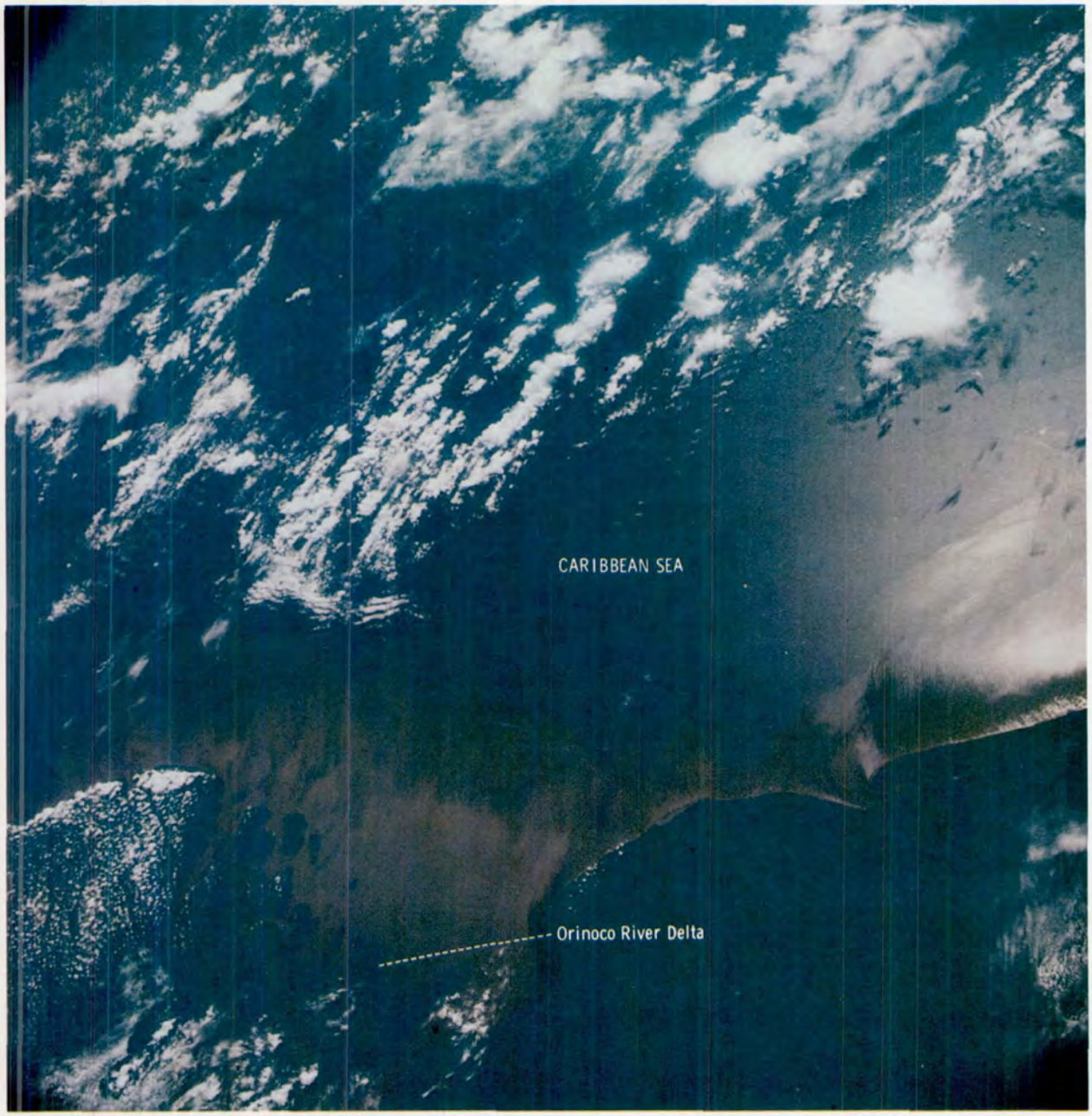

Figure 10-7.- The deep-brown color of the Orinoco River outflow is caused by both sediments and humic compounds. This turbid water was observed by the crew farther north than the island of Barbados (AST-21-1685).

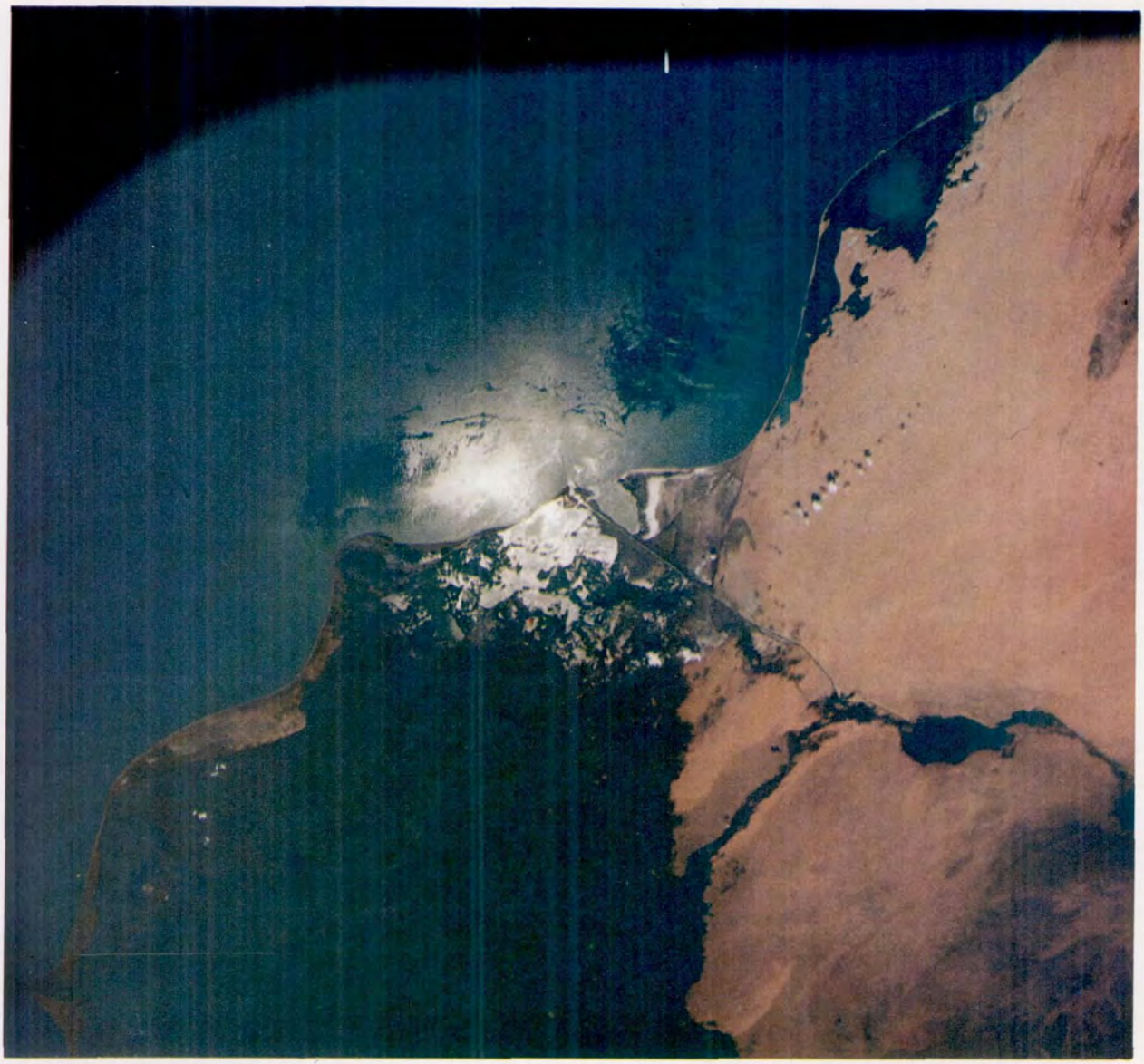

Figure 10-8.- The Nile Delta is an excellent example of a triangular-shaped arcuate delta. Patterns of surface texture and boundary layers, easily seen in the Sun's reflection, possibly result from a density difference between the freshwater from the Nile and the more saline water of the Mediterranean Sea (AST-9-558).

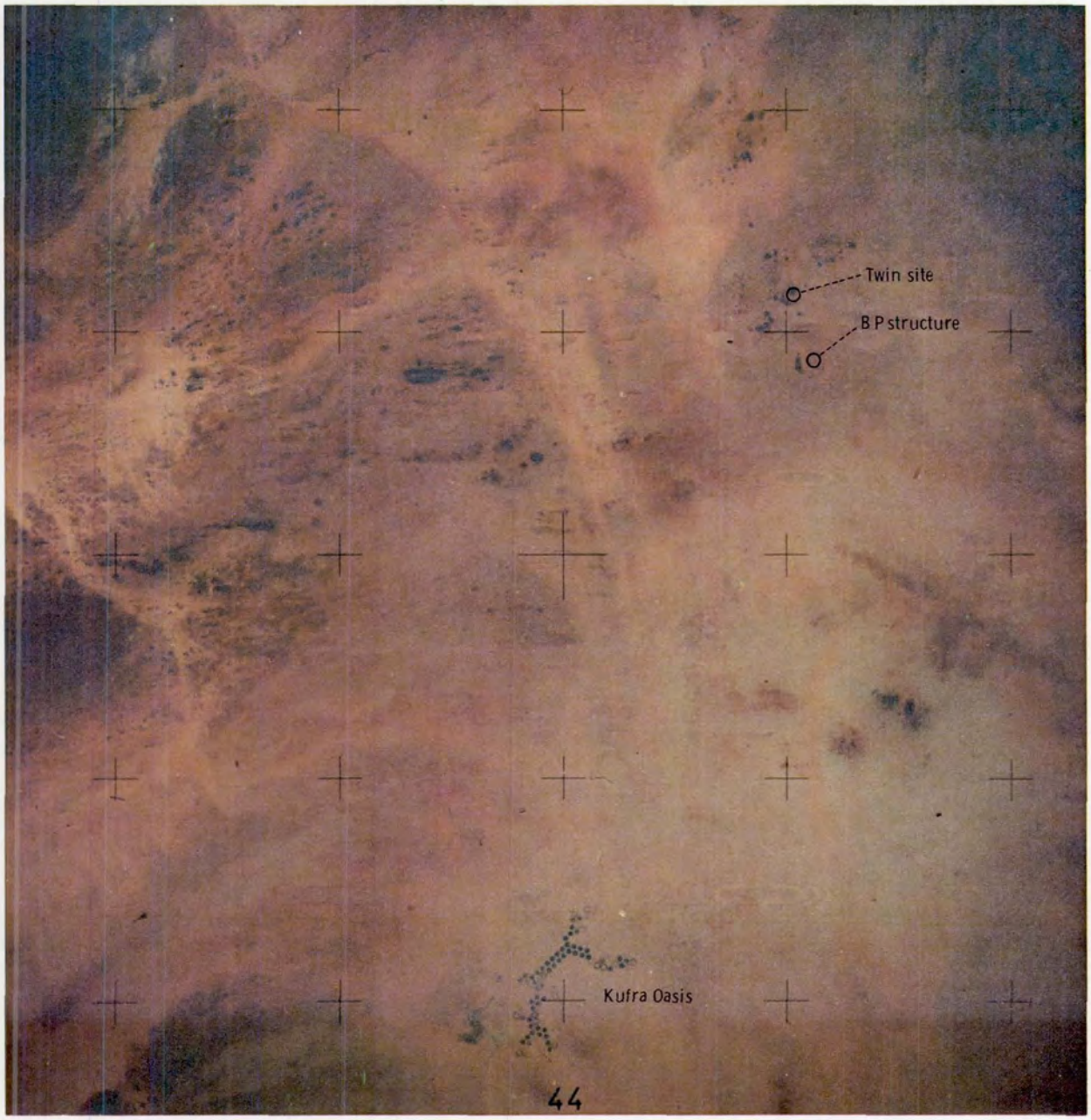

Figure 10-9.- The Kufra Oasis, in the lower half of the photograph, is characterized by circular irrigation patterns. To the north, two faint rings (arrows) are possible astroblemes (AST-16-1244).

(a) The Atlantic Ocean appears homogeneous with no visible ocean features in this oblique photograph looking toward the Strait of Gibraltar (AST-27-2365).

Figure 10-10.- The Strait of Gibraltar.

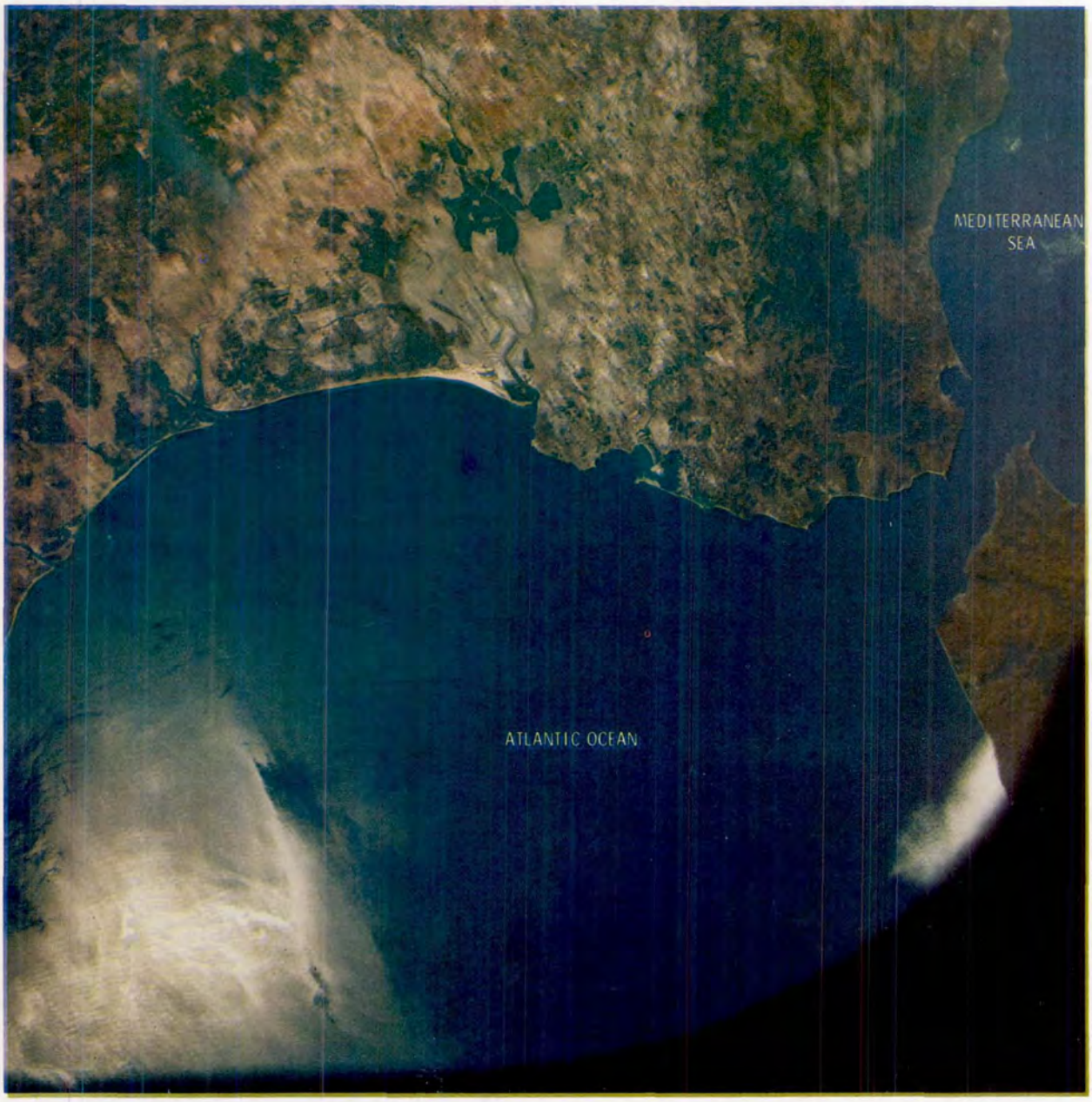

(b) The change in Sun angle in this photograph, taken shortly after figure 10-10(a), has made a number of features visible. Orbital photography of the oceans has revealed that the occurrence and magnitude of internal waves is greater than expected. The internal waves in this photograph are approximately 50 to 60 kilometers long (AST-27-2367).

Figure 10-10.- Concluded.

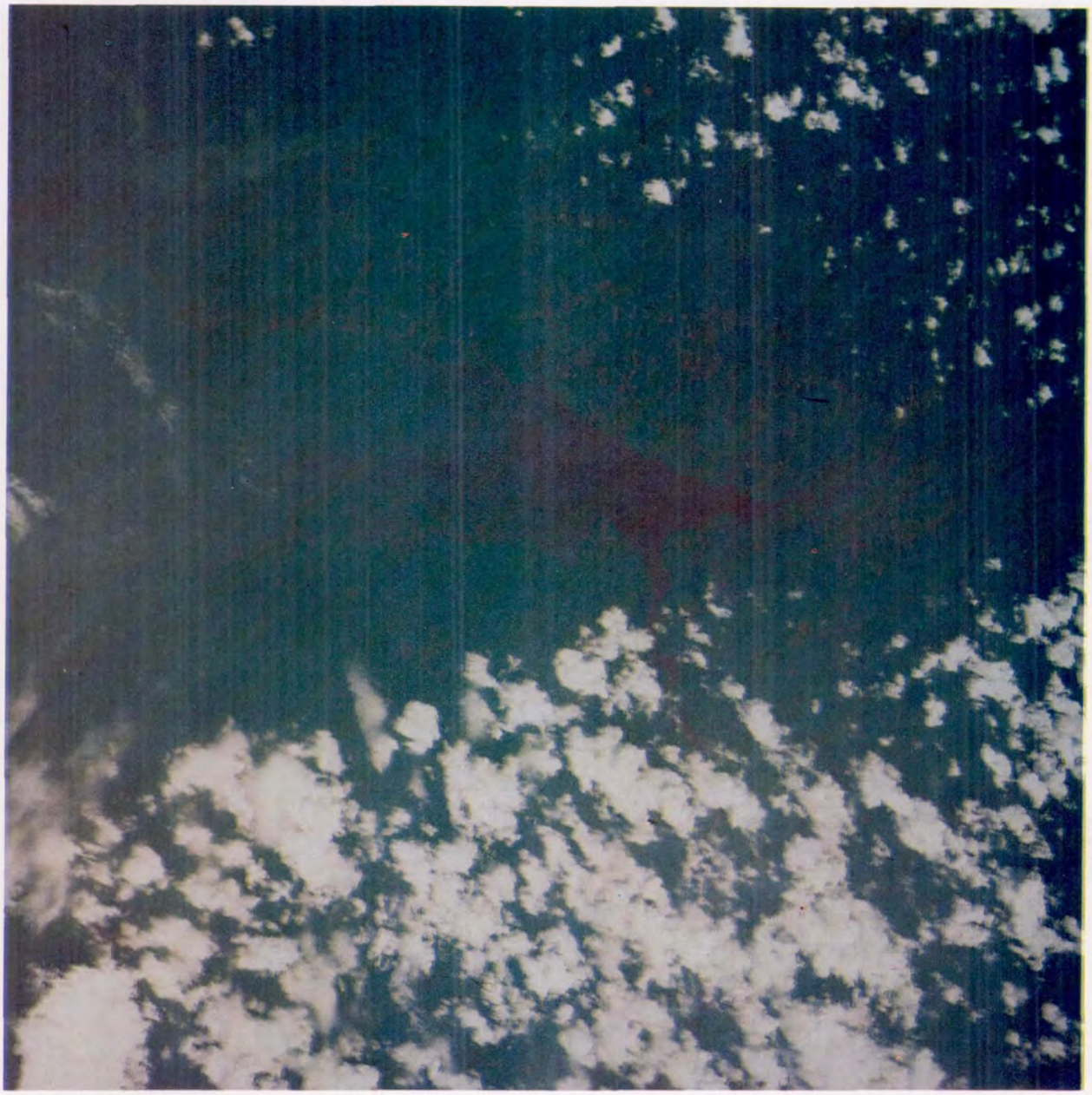

Figure 10-11.- In this photograph of the Bay of Fundy, the red water color is probably due to the deposition of red clays by inflowing rivers. There is a fairly heavy sediment load in the bay; high tidal activity maintains water turbulence (AST-1-67).

Figure 10-12.- This vertical photograph was taken with the mapping camera over the Western Desert of Egypt. A sharp color change marks the boundary between the younger, yellow sand sea to the north and the older, orange-red desert associated with the Gilf el Kebîr region in the lower part of the photograph (AST-16-1247).

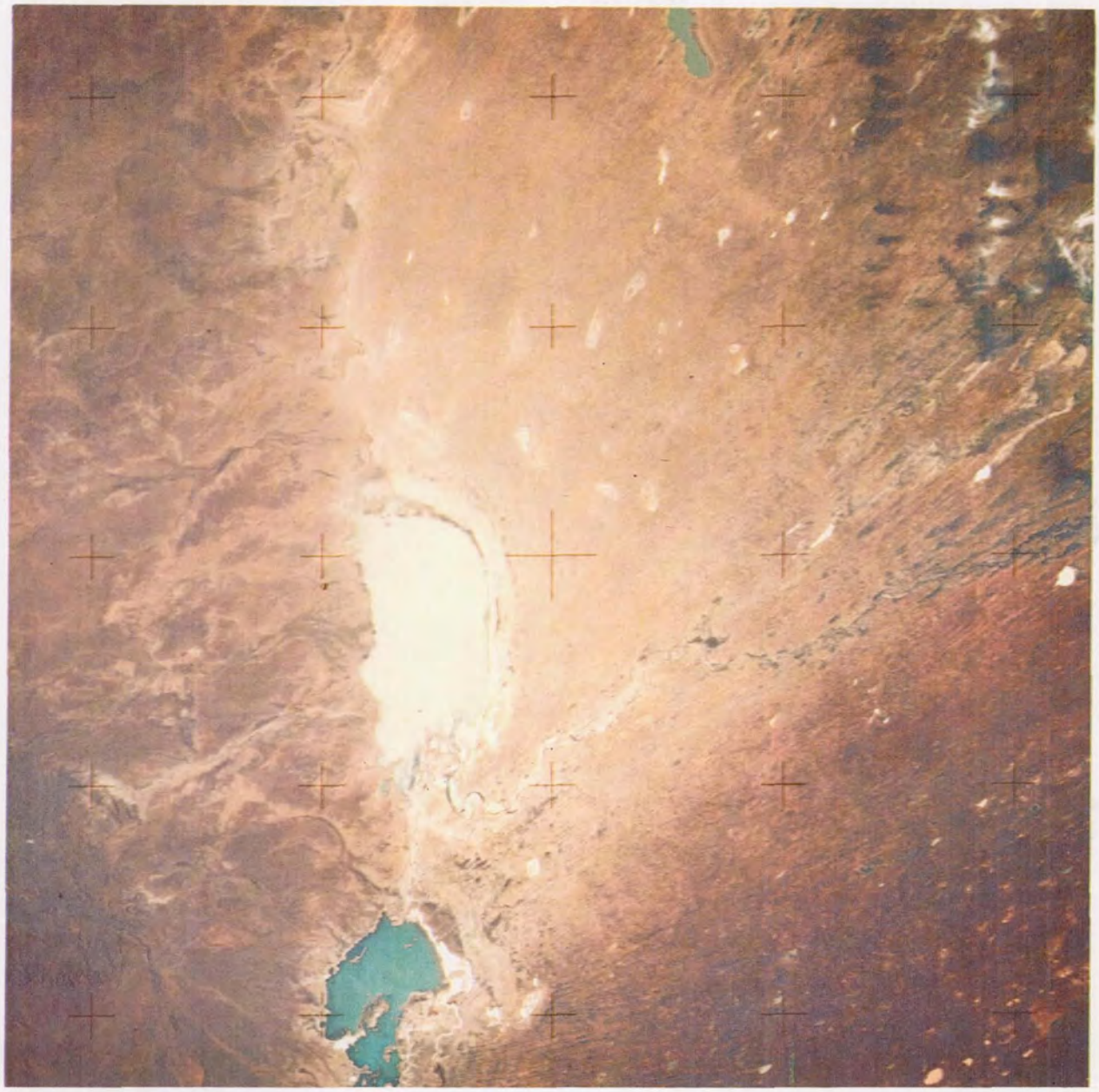

Figure 10-13.- The color difference between the dark-red Simpson Desert and the yellow Western Desert of Egypt in figure 10-12 is readily apparent. The radiating linear dunes in this photograph, described by the crew as "hundreds of parallel road tracks," seem to constitute the characteristic dune pattern in this region (AST-16-1133).

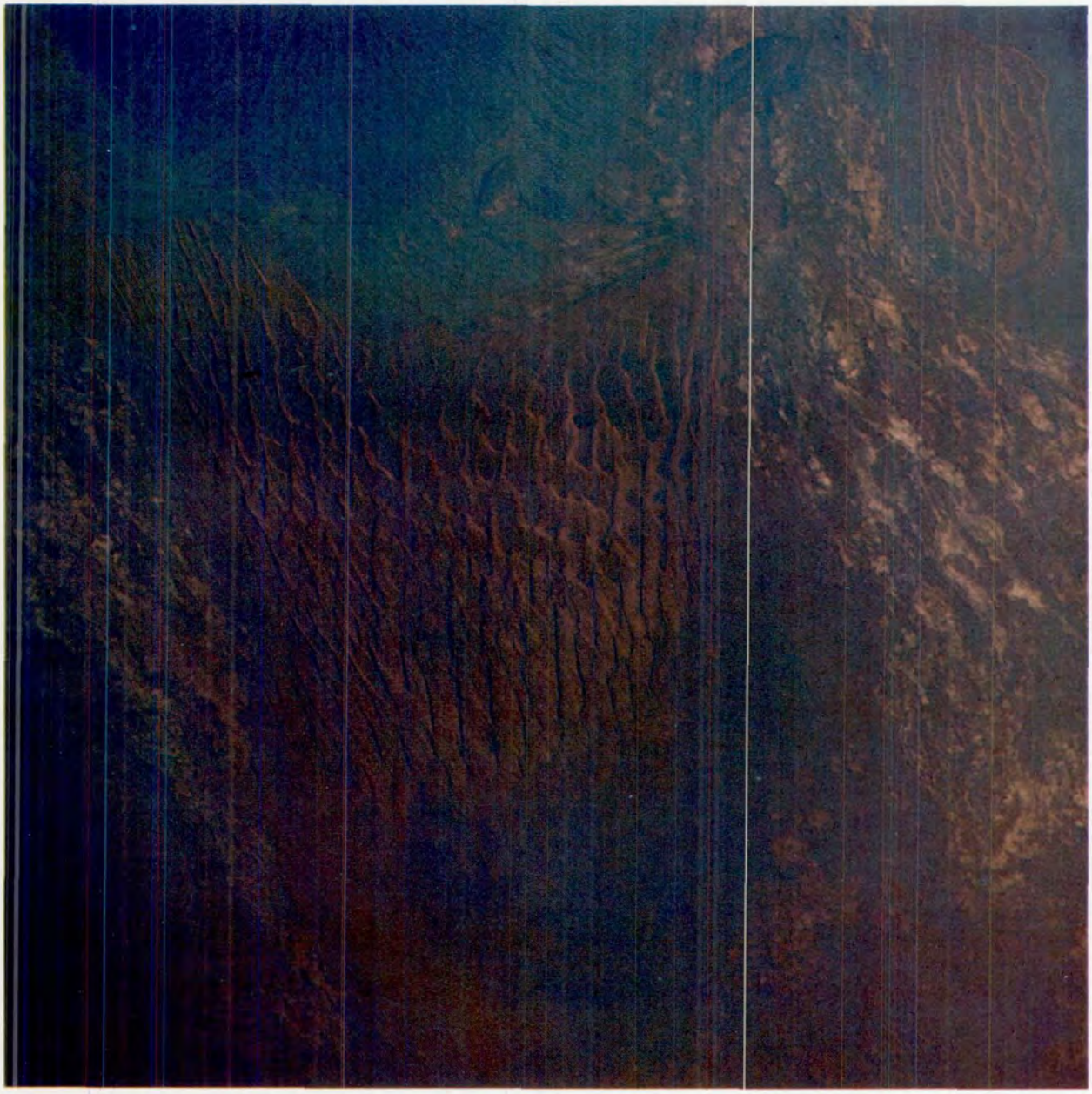

Figure 10-14.- In this excellent photograph of a little-known dune field in Argentina, the transition between the alluvial fan at the base of the mountain and the dune field is very sharp. The general dune pattern is crescentic with a superimposed secondary linear pattern. To the east of the dune field is a smaller field, the existence of which was previously unknown (AST-27-2340).

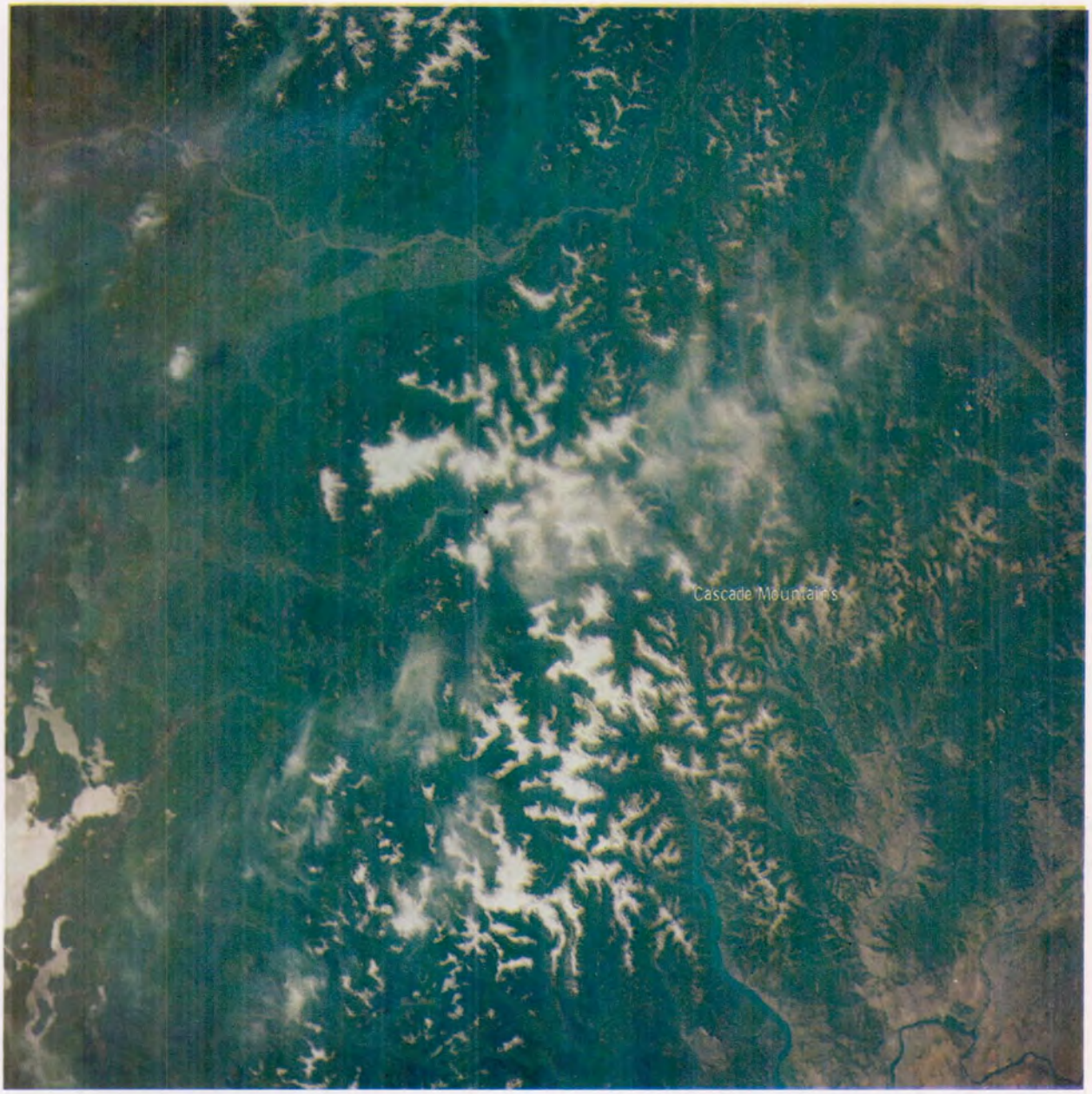

Figure 10-15.- This photograph of the July snow cover was taken over the Cascades in the State of Washington. Snowpack distribution is being mapped to estimate the volume of water reaching drainage systems for use in irrigation (AST-19-1540).

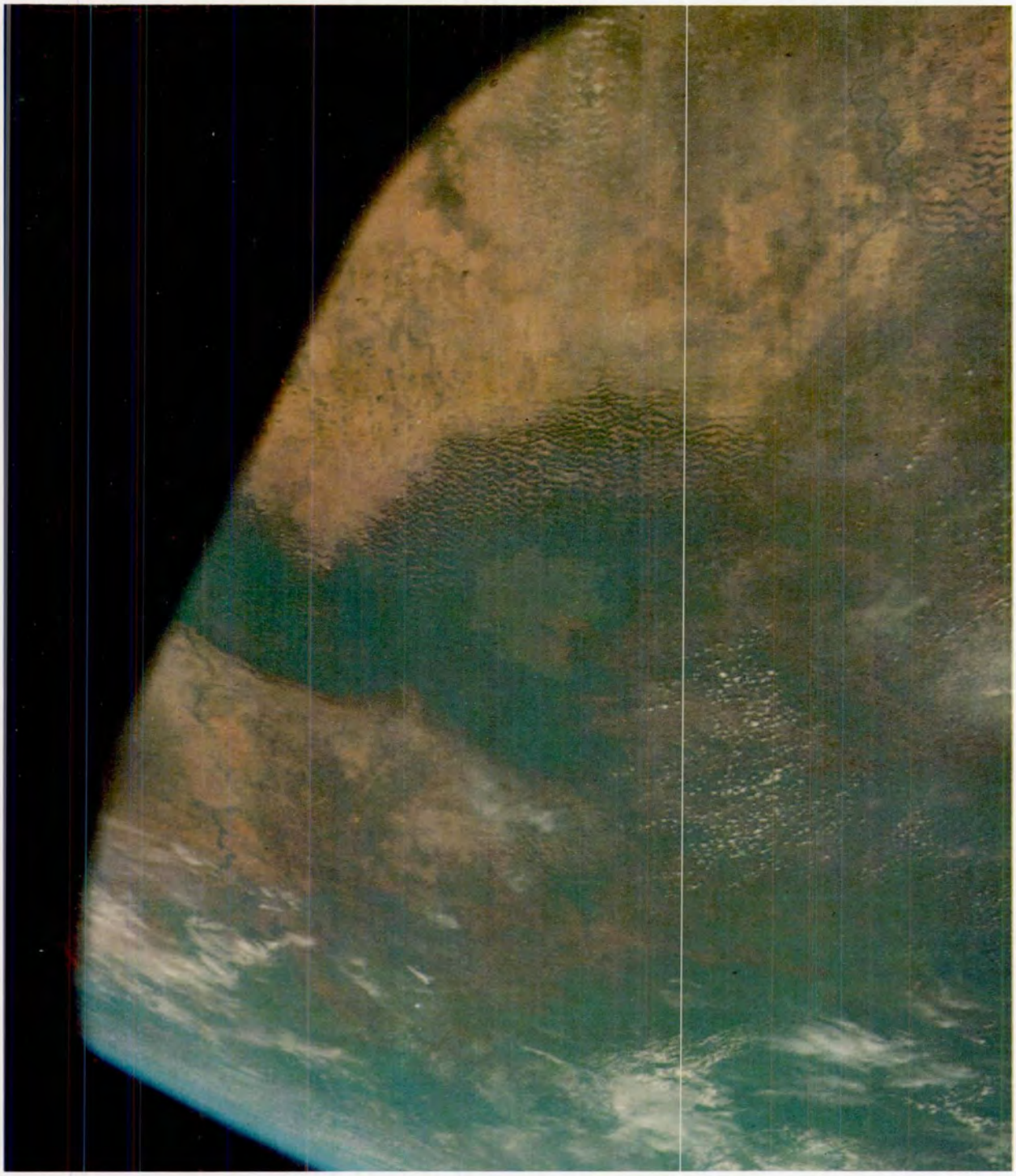

Figure 10-16.- In this photograph of Lake Chad, the number of emergent dunes within the lake attest to the fact that the lake was once considerably larger. However, various factors, such as the influx of sand from the Sahara, have contributed to a significant decrease in its size (AST-9-550).

Figure 10-17.- This photograph of an unusual cumulonimbus convective system was taken along the western coast of Mexico over the Gulf of California (AST-9-545).

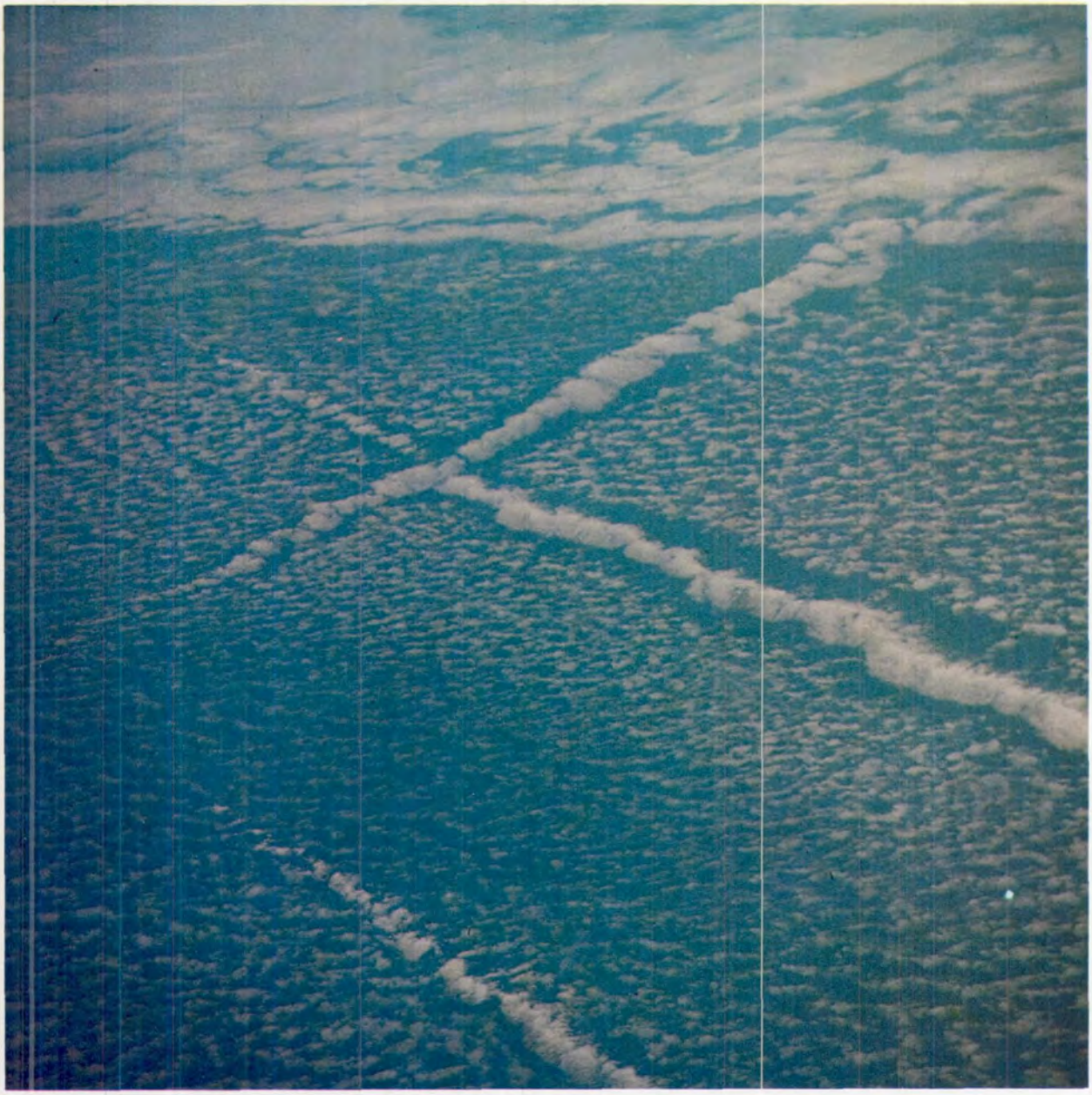

Figure 10-18.- The unique, wedge-shaped linear features in this photograph taken over the Pacific Ocean west of southern California are significantly larger than contrails. Their mode of formation is not yet understood (AST-1-42).

APPENDIX A

ABBREVIATIONS AND ACRONYMS

ac	alternating current
ACDR	Apollo commander
A-D	analog to digital
amu	atomic mass unit
ANZUS	Australia-New Zealand-United States
ASTP	Apollo-Soyuz Test Project
at.%	atomic percent
ATS	Applications Technology Satellite
ATSR	Applications Technology Satellite ranging
BTB	bromthymol blue agar
CF	cryogenic freezer
CGE	Crystal Growth Experiment
CM	command module
CMC	command module computer
CMMY	corn-meal, malt-extract, yeast-extract agar
CMP	command module pilot
CN	cellulose nitrate
COAS	crew optical alinement sight
Co-I	Co-Investigator
Con A	Concanavalin A
CPM	counts per minute
CSM	command and service module
CTA	cellulose triacetate
D-A	digital to analog
DAC	data acquisition camera
dc	direct current
D/L	diameter to length ratio
DM	docking module
DMA	Defense Mapping Agency
DMP	docking module pilot
DNA	deoxyribonucleic acid
DTA	differential thermal analysis
ECE	electrical checkout equipment
ECS	environmental control system
EMI	electromagnetic interference
EPE	Electrophoresis Experiment
EU	electrophoresis unit
EUV	extreme ultraviolet
FCS	fetal calf serum
FOV	field of view
FWHM	full width, half maximum
GBT	ground-based test
GEM	Goddard Earth Model
GET	ground elapsed time
GMT	Greenwich mean time
HDC	Hasselblad data camera

HED	high-energy deposition
HeG	helium glow
HGD	helium glow detector
HRC	Hasselblad reflex camera
HVPS	high-voltage power supply
HZE	high-charge energy
ICRP	International Commission for Radiation Protection
IF	intermediate frequency
IR	infrared
ISM	interstellar medium
JSC	NASA Lyndon B. Johnson Space Center
KSC	NASA John F. Kennedy Space Center
LaRC	NASA Langley Research Center
LBL	Lawrence Berkeley Laboratory
LED	light-emitting diode
LeRC	NASA Lewis Research Center
LET	linear energy transfer
LFE	Light Flash Experiment
lidar	laser radar
MEM	minimum essential medium
NOAA	National Oceanic and Atmospheric Administration
NRL	Naval Research Laboratory
OM	orbital module
PBS	phosphate-buffered saline
PGS	preliminary Goddard solution
PHA	phytohemagglutinin
PI	Principal Investigator
PMN	polymorphonuclear leukocyte
PVA	polyvinylalcohol
PWM	pokeweed mitogen
QT	quantum efficiency and transmission
RBE	relative biological effectiveness
RCS	reaction control system
RF	radiofrequency
RPI	Rensselaer Polytechnic Institute
SAA	South Atlantic Anomaly
SAB	Sabouraud's dextrose agar
SAM	stratospheric aerosol measurement
SAO	Smithsonian Astrophysical Observatory
SAS	small astronomy satellite
SCDR	Soyuz commander
SD	standard deviation
SEM	scanning electron microscope
SF	space flight
SFE	Soyuz flight engineer
SI	simulation index
SIM	scientific instrument module
SM	service module
SRBC	sheep red blood cells
SST	supersonic transport or satellite-to-satellite tracking
STDN	Spaceflight Tracking and Data Network

TE	thermoelectric module
TLD	thermoluminescence dosimeter
TV	thermal vacuum or television
UK	urokinase
USB	unified S-band
UVA	ultraviolet absorption
VCO	voltage-controlled oscillator
VHF	very high frequency
VTR	video tape recorder
WBC	white blood cell
wt.%	weight percent
XBT	expendable bathythermograph
Z	atomic number
ZFF	zone-forming fungi

APPENDIX B

UNITS AND UNIT-CONVERSION FACTORS

In this appendix are the names, abbreviations, and definitions of International System (SI) units used in this report and the numerical factors for converting from conventional units to SI units.

Names and Symbols of SI Units

Quantity	Name of unit	Symbol	Definition of symbol
	SI Base Units		
Length	meter	m	
Mass	kilogram	kg	
Time	second	sec	
Electric current	ampere	A	
Thermodynamic temperature	kelvin	K	
Luminous intensity	candela	cd	
Amount of substance	mole	mol	
	SI Derived Units		
Area	square meter	m^2	
Volume	cubic meter	m^3	
Frequency	hertz	Hz	s^{-1}
Mass density (density)	kilogram per cubic meter	kg/m^3	
Speed, velocity	meter per second	m/sec	
Angular velocity	radian per second	rad/sec	
Acceleration	meter per second squared	m/sec^2	
Angular acceleration	radian per second squared	rad/sec^2	
Force	newton	N	$kg \cdot m/sec^2$
Pressure (mechanical stress)	pascal	Pa	N/m^2
Kinematic viscosity	square meter per second	m^2/sec	
Dynamic viscosity	newton-second per square meter	$N \cdot sec/m^2$	
Work, energy, quantity of heat	joule	J	$N \cdot m$
Power	watt	W	J/sec
Quantity of electricity	coulomb	C	$A \cdot sec$
Potential difference, electromotive force	volt	V	W/A
Electric field strength	volt per meter	V/m	
Electric resistance	ohm	Ω	V/A
Capacitance	farad	F	$A \cdot sec/V$
Magnetic flux	weber	Wb	$V \cdot sec$
Inductance	henry	H	$V \cdot sec/A$
Magnetic flux density	tesla	T	Wb/m^2
Magnetic field strength	ampere per meter	A/m	
Magnetomotive force	ampere	A	
Luminous flux	lumen	lm	$cd \cdot sr$
Luminance	candela per square meter	cd/m^2	
Illuminance	lux	lx	lm/m^2
Wave number	1 per meter	m^{-1}	
Entropy	joule per kelvin	J/K	
Specific heat capacity	joule per kilogram kelvin	$J/(kg \cdot K)$	
Thermal conductivity	watt per meter kelvin	$W/(m \cdot K)$	
Radiant intensity	watt per steradian	W/sr	
Activity (of a radioactive source)	1 per second	s^{-1}	
	SI Supplementary Units		
Plane angle	radian	rad	
Solid angle	steradian	sr	

Unit Prefixes

Prefix	Abbreviation	Factor by which unit is multiplied
giga	G	10^{9}
mega	M	10^{6}
kilo	k	10^{3}
centi	c	10^{-2}
milli	m	10^{-3}
micro	μ	10^{-6}
nano	n	10^{-9}
pico	p	10^{-12}

Unit Conversion Factors

The following table expresses the definitions of units of measure used in the Apollo-Soyuz Test Project Preliminary Science Report as exact numerical multiples of coherent SI units and provides multiplying factors for converting to SI units. The first two digits of each numerical entry represent a power of 10. An asterisk follows each number which expresses an exact definition.

To convert from -	To -	Multiply by -
angstrom	meter	-10 1.00*
atmosphere	newton/meter^2	+05 1.013 25*
Celsius (temperature)	kelvin	$t_K = t_C + 273.15$
foot	meter	-01 3.048*
gram	kilogram	-03 1.00*
inch	meter	-02 2.54*
pound mass (lbm avoir-dupois)	kilogram	-01 4.535 923 7*
torr (0° C)	newton/meter^2	+02 1.333 22

APPENDIX C

HARDWARE VENDORS

Experiment	Equipment supplied	Vendor
Microbial Exchange (AR-002)	Experiment hardware	General Electric Company Houston, Tex.
Stratospheric Aerosol Measurement (MA-007)	Experiment hardware	University of Wyoming Laramie, Wyo.
Multipurpose Electric Furnace (MA-010)	Experiment hardware	Westinghouse Astronuclear Pittsburgh, Pa.
Electrophoresis Technology (MA-011)	Experiment hardware	Teledyne Brown Engineering Huntsville, Ala.
	Thermoelectric assembly	Ohio Semitronics Columbus, Ohio
	Column assemblies	NASA George C. Marshall Space Flight Center Huntsville, Ala.
Electrophoresis (MA-014)	Experiment hardware	Messerschmitt-Bölkow-Blohm Ottobeuren, West Germany
Crystal Growth (MA-028)	Experiment hardware	Rockwell International Science Center Thousand Oaks, Calif.
	Camera equipment and accessories	NASA Lyndon B. Johnson Space Center Houston, Tex.
Soft X-ray Observation (MA-048)	Experiment and ground-support equipment (GSE)	Ball Brothers Research Corporation Boulder, Colo.
	Data subsystem	New Mexico State University Las Cruces, N. Mex.
Ultraviolet Absorption (MA-059)	Experiment, optical system, and GSE	Johns Hopkins University Applied Physics Laboratory Laurel, Md.
	Retroreflector optics (built and tested)	Precision Lapping and Optical Company Valley Stream, N.Y.
	Ultraviolet (UV) light source (built)	Intraspace International Inc. Toronto, Ontario, Canada
	UV light assembly (design and assembly)	Lockheed Electronics Houston, Tex.
	Retroreflector mount, UV and incandescent light sources, and GSE	NASA Lyndon B. Johnson Space Center Houston, Tex.
Extreme Ultraviolet Survey (MA-083)	Experiment and GSE	Ball Brothers Research Corporation Boulder, Colo.
	Telescope	Applied Optics Center Burlington, Mass.
	UV filters	Luxel Corporation Santa Barbara, Calif.

Experiment	Equipment supplied	Vendor
Interstellar Helium Glow (MA-088)	Experiment and GSE	Ball Brothers Research Corporation Boulder, Colo.
	Helium pressure vessel	Supplied by NASA
	Helium system valves	Sterer Valves Engineering & Manufacturing Los Angeles, Calif.
	UV filters	Luxel Corporation Santa Barbara, Calif.
Doppler Tracking (MA-089)	Transmitter, receiver, and GSE	Raytheon Company Equipment Division Sudbury, Mass.
	Ultrastable oscillators for transmitters and receivers, crystal filters for transmitters	Frequency Electronics, Inc. New Hyde Park, N.Y.
	Transmitter battery development	Eagle Picher Joplin, Mo.
	Receiving antenna (design and development)	Ball Brothers Research Corporation Boulder, Colo.
	Data recording system	NASA Lyndon B. Johnson Space Center Houston, Tex.
Light Flash (MA-106)	Experiment hardware	Lawrence Livermore Laboratory University of California Berkeley, Calif.
Biostack (MA-107)	Experiment hardware	Messerschmitt-Bölkow-Blohm Ottobeuren, West Germany
Earth Observations and Photography (MA-136)	70-mm cameras, magazines, lenses, and accessories for photography	Victor Hasselblad, Aktiebolag Sweden
	20X binoculars for visual observations	Tasco Sales, Inc. Miami, Fla.
	Standard color chips for visual color comparisons	Munsell Color Company Macbeth Division Baltimore, Md.
	Zoom telescope for visual observations	Bushnell Optical Corporation Pasadena, Calif.
	Variable intervalometer for sequencing photography; 16-mm camera equipment for complementary strip mapping	Perkin Elmer Corporation Aerospace Division Pomona, Calif.
Crystal Activation (MA-151)	Experiment hardware	NASA Goddard Space Flight Center Greenbelt, Md.
Science Demonstrations	Experiment hardware	NASA George C. Marshall Space Flight Center Huntsville, Ala.

APPENDIX D

POINTS OF CONTACT

Experiment no.	Engineering development manager	Science coordinator
NASA Lyndon B. Johnson Space Center		
AR-002	--	G. R. Taylor, DD7
MA-007	--	J. R. Bates, TN3
MA-028	C. J. LeBlanc, ED6	J. R. Bates, TN3
MA-031	--	S. L. Kimzey, DB7
MA-032	--	S. L. Kimzey, DB7
MA-048	E. L. Weeks, ED6	S. N. Hardee, TN3
MA-059	L. W. McFaden, ED6	S. R. Mansur, TN3
MA-083	J. M. Sanders, ED6	R. R. Baldwin, TN3
MA-088	J. M. Sanders, ED6	R. R. Baldwin, TN3
MA-089	A. R. Cunningham, EE6, and J. S. Kelley, EE3	P. E. Lafferty, TN3
MA-106	J. D. Lem, DE4	R. A. Hoffman, DD6
MA-107	H. S. Anton[a]	J. V. Bailey, DD6
MA-128	--	P. E. Lafferty, TN3
MA-147	--	G. R. Taylor, DD7
MA-148	--	R. T. Giuli, TN3
MA-151	--	S. R. Mansur, TN3
MA-161	--	R. A. Hoffman, DD6
NASA George C. Marshall Space Flight Center		
MA-010	A. Boese, EL55	A. Boese, EL55
MA-011	R. E. Allen, EH35	R. E. Allen, EH35
MA-014	R. S. Snyder, EH12	R. S. Snyder, EH12
MA-041	A. Boese, EL55	R. C. Ruff, ES12
MA-044	A. Boese, EL55	L. L. Lacy, ES24
MA-060	A. Boese, EL55	C. F. Schafer, ES12
MA-070	A. Boese, EL55	C. S. Griner, EH12
MA-085	A. Boese, EL55	M. C. Davidson, ES12
MA-131	A. Boese, EL55	M. H. Johnston, EH12
MA-150	A. Boese, EL55	A. Boese, EL55

[a]Ministry of Research and Technology, Federal Republic of Germany, Gesellschaft Fuer Weltraumforschung, 505 Porz-Wahn, Linder Hoehe, West Germany.

☆ U.S. GOVERNMENT PRINTING OFFICE 1976—0—675—606